이학 박사학위논문

Influence of Inflammation on Bone Regeneration of Dental Stem Cells: Role of TGF-β2/BMP-2

염증반응이 치아줄기세포의 골재생에 미치는 영향 - TGF-β2/BMP-2 의 역할

2017 년 8 월

서울대학교 대학원
치의과학과 치의재생생명공학 전공

엄 소 연

Influence of Inflammation on Bone Regeneration of Dental Stem Cells: Role of TGF-β2/BMP-2

염증반응이 치아줄기세포의 골재생에 미치는 영향
－ TGF－β2/BMP－2 의 역할

지도교수 서 병 무

이 논문을 이학 박사학위논문으로 제출함
2017 년 4 월

서울대학교 대학원
치의과학과 치의재생생명공학 전공

엄 소 연

엄소연의 박사학위논문을 인준함
2017 년 6 월

위 원 장 _____ (인)

부위원장 _____ (인)

위 원 _____ (인)

위 원 _____ (인)

위 원 _____ (인)

- Abstract -

Influence of Inflammation on Bone Regeneration of Dental Stem Cells: Role of TGF-β2/BMP-2

Soyoun Um

Program in Dental Regenerative Biotechnology,

Department of Dental Science,

Graduate School, Seoul National University

(Directed by Professor **Byoung Moo Seo**, D.D.S., M.S.D., Ph.D.)

1. Purpose

Bone formation is important for reconstructing the bone-related structure in areas damaged by inflammation. Inflammatory conditions inhibits osteoblastic differentiation, as shown in rheumatoid arthritis, cystic fibrosis, and periodontitis. In this study, periodontal ligament stem cells (PDLSCs), bone marrow stem cells from the maxilla (BMSCs), and dental follicle stem cells (DFSCs), as known for

mesenchymal stem cells (MSCs), were used to demonstrate the relationship between inflammation and osteogenesis.

2. Materials and methods

Human PDLSCs and BMSCs are MSCs obtained from the periodontal ligament of extracted third molars and from bone marrow of the maxilla, respectively. Osteogenic differentiation was measured by ALP activity and alizarin red S staining. Proteins were assessed by flow cytometry, ELISA, western blotting, and immunocytochemistry. Changes of gene expression were measured by RT-PCR and real-time PCR.

DFSCs, founded in developing tooth germ, were tested in conjunction with the role of TGF-β2 in the relationship between an inflammatory environment and bone formation. Protein analysis was performed by liquid chromatography coupled with tandem mass spectrometry to analyze the difference between inflamed and normal tissue.

3. Results

[Part 1]

A high BMP-2 concentration inhibited the early stages of osteogenesis in MSCs. Also, co-culturing THP-1 with MSCs suppressed the late stages of osteogenesis. In addition, high-dose BMP-2 induced inflammatory cytokines in THP-1 cells; and the anti-inflammatory cytokine TSG-6 in MSCs. IL-1β expression was downregulated by TSG-6 treatment of THP-1 cells. TSG-6 secreted by MSCs suppressed inflammatory reactions through p38 and ERK in the mitogen-activated protein kinase (MAPK) pathway.

[Part 2]

In inflamed DFSCs, ALP activity and alizarin red S staining were decreased in the presence of osteogenic differentiation. Also, *in vivo* transplantation showed severe impairment of osteogenesis in inflamed DFSCs. Protein profile analysis showed that TGF-β1 and TGF-β2 have different expressions in inflamed DFSCs. Osteogenic differentiation was suppressed in LPS-treated DFSCs due to a low level of TGF-β1 and high level of TGF-β2. TGF-β2 inhibitors increased osteogenesis in DFSCs. Moreover, TGF-β1 expression was also increased with inhibition of TGF-β2.

4. Conclusions

In conclusion, an inflammatory environment affects the osteogenic differentiation

on MSCs. MSCs in inflammatory conditions have the low osteogenic differentiation potentials, caused by TGF-β2. Also, MSCs triggered by inflammatory conditions secreted the anti-inflammatory cytokine, TSG-6, to inhibit inflammatory reactions and increase osteogenic differentiation. Understanding the relationship between inflammation and bone formation in MSCs is important in regenerative medicine and for the future clinical use of dental stem cells.

Keywords: periodontal ligament stem cells, bone marrow stem cells, dental follicle stem cells, bone regeneration, inflammation, BMP-2, TSG-6, TGF-β2

Student Number: 2011-23827

Table of Contents

Introduction

Tissue regeneration with stem cells is a promising field in regenerative medicine. Among candidate stem cells for tissue regeneration, mesenchymal stem cells have potential clinical applications. Regeneration of tissue defects in the oral cavity is challenging because of the complex composition and multiple cell types in this area. After a diseased tooth or bone is removed, the defective surrounding bone must be primarily regenerated[1].

Bone regeneration is critical for reconstructing the bone structure destroyed by pathologic processes or traumatic causes. In general, mesenchymal stem cells are recruited to the site of destruction to regenerate damaged bone. However, bone formation near a destructed area is influenced by local inflammatory condition and degree of tissue injuries. Bone-related diseases induce the inflammatory environment that might inhibit osteoblastic differentiation and bone formation, as demonstrated in rheumatoid arthritis, cystic fibrosis, and periodontitis[2, 3].

Characteristics of mesenchymal stem cells

Mesenchymal stem cells (MSCs) were found in 1924 by Alexander A. Maximow by identifying the precursor cell in mesenchyme that differentiated

into different blood cells[4]. Through many studies of MSCs, different sources of MSCs were discovered and comprise; bone marrow, cord cells, adipose tissue, and molar tooth cells[1, 5-7]. Recently, MSCs from dental follicles, periodontal ligament, and bone marrow were isolated and differentiated into clonogenic, plastic-adherent, and fibroblast-like cells[8, 9 10, 11]. MSCs found in various dental tissues are also considered as potential stem cell sources[10, 12]. The multipotency of dental stem cells has a potential to reconstruct the bone structure in an inflammatory condition[13-16]. As one of the common diseases causing tooth loss, periodontal disease is defined as destruction of alveolar bone and periodontal tissues by bacterial infection[13, 14, 17]. Therapeutic strategies for the treatment of periodontitis include not only control of local inflammation, but also regeneration of new periodontal tissues attached to the surface of the tooth root. Among MSCs of dental origin, periodontal ligament stem cells (PDLSCs), which are obtained from extracted third molars, have been identified and characterized as a multipotent stem cell that can be used for hard tissue regeneration[18, 19]. Another candidate for bone regeneration is bone marrow stem cells (BMSCs)[1, 20]. Dental follicles, derived from ectomesenchymal origin, surround the developing tooth germ and contain the periodontal precursor cells that give rise to periodontal tissue of cementum, periodontal ligament, and alveolar bone during tooth development[21-23]. Dental

follicle stem cells (DFSCs) are also possible candidates for use in hard tissue regeneration.

Effects of bone morphogenetic protein on bone formation and inflammation

Human bone morphogenetic protein-2 (BMP-2), a growth factor, is important for development of bone and cartilage[24]. Many studies showed that BMP-2 is involved in the hedgehog pathway, TGF beta signaling pathway, and in cytokine-cytokine receptor interactions. BMP-2 has been approved by the United States Food and Drug Administration (FDA) for use in bone regeneration and repair and is used at 0.5-1 mg/ml in autogenous bone grafts, spinal fusion, segmental defects, open tibia fractures, and maxillofacial reconstruction with a variety of biomaterial carriers[25-30]. Unlike an *in vitro* study of 50-200 ng/ml BMP-2[31], the clinical dosages of BMP-2 are extremely high. In the first clinical reports of 1 mg/ml BMP-2 use, several adverse effects were reported[32-36]. High BMP-2 concentrations increase osteoclast activation with transient bone resorption[37]. A frequently reported side effect of BMP-2 is inflammatory swelling. Patients undergoing anterior cervical spinal fusion generally exhibit severe soft tissue swelling and require surgery to explore and drain a swollen anterior neck with transplantation of rhBMP-2

sponges[38]. Several reports also noted catastrophic complications, ectopic growth, decreased protein delivery, and inactivation of protein with use of BMP-2 in spinal fusion surgeries[39].

Previous research reported that BMP-2 triggers chemotaxis of monocytes, macrophages, and lymphocytes[40-42]. In inflammation and bone formation, inflammatory cytokines triggered by immune cells not only sustain inflammation, but also activate bone resorption in osteoporosis, rheumatoid arthritis, and other bone diseases[3, 43]. The inflammatory mechanisms acting between immune cells and hMSCs in bone formation have been investigated *in vivo*. With high doses of BMP-2, infiltrated immune cells, inducing inflammatory cytokines, were increased near the transplanted area and formed aberrant bone[32, 44]. To reduce life-threatening episodes and increase bone formation, the optimum BMP-2 concentration needs to be determined, and the inflammatory environment induced by BMP-2 needs to be controlled. Moreover, establishing these conditions will elucidate the interactions between immune cells and hMSCs. However, the role of hMSCs on BMP-2 induced inflammation is not known.

Effects of the transforming growth factor-beta family on bone formation and inflammation

Transforming growth factor-beta (TGF-β), a secreted protein with four different isoforms TGF-β 1 to 4, is involved in various signaling pathways. By binding the TGF-β receptors, composed of both type 1 and type 2 receptor subunits, the type 2 receptor kinase phosphorylates and then activates type 1 receptor kinase to activate a signaling pathway. TGF-β triggers the downstream of differentiation, proliferation, and activation various immune cells[45, 46].

TGF-β also has multiple roles in both osteogenesis and immune-regulation[47-49]. However, conflicting results of the effects of TGF-β on bone formation were reported. TGF-β controls bone formation by modulating osteoblastic cell proliferation and differentiation *in vitro*. TGF-β also regulates inflammation by suppressing pro-inflammatory cytokines[50, 51]. In contrast, TGF-β suppressed osteogenesis in murine cell lines and human MSCs *in vitro*[52-54]. These controversial results might be related with confusing use of TGF-β without discrimination of TGF-β1 and β2. We focused on the distinct functions of TGF-β1 and TGF-β2 in osteogenesis and inflammatory conditions.

Exogenous TGF-β2 reduces bone and cartilage formation in healing fractures in rabbits[55]. Comparison of the expression patterns of TGF-β1 and TGF-β2 in human bone samples showed that TGF-β2 was highly enhanced in

osteoarthritic bone compared to normal bone, in contrast to TGF-β1[56]. These results suggested that TGF-β2 could have a complex role in bone formation during inflammatory conditions.

Porphyromonas gingivalis (*P.g.*) is a Gram-negative bacterium frequently found in oral tissue. *P.g.*- derived lipopolysaccharide (LPS) is a crucial virulent factor etiologically associated with initiation and development of periodontal disease[57, 58]. It has been reported that *P.g.*-derived LPS acts as a potent stimulator of inflammatory cytokine production and bone resorption[59]. However, the exact mechanisms and connections between infectious disease and bone formation are unclear. Until now, little was known about the relationship between an inflammatory environment and down-regulation of bone formation. A previous study showed that the toll-like receptors, TLR2 and TLR4, are stimulated by LPS, while LPS sensing triggered cell viability and cytokine secretion of MSCs[60]. Also, direct contact with bacterial toxins on MSCs triggered immune responses. Patients with periodontitis have symptoms such as gingival bleeding and progressive alveolar bone destruction. Therefore, it is necessary to clarify the inter-relationship between bone formation and inflammation.

Anti-inflammatory effects of mesenchymal stem cells

Recent reports have demonstrated that MSCs regulate inflammation[61-65]. In addition to the capacity to differentiate into cell types such as adipocytes, osteoblasts, and neurons, hMSCs also have immunomodulatory characteristics[66]. Some studies discovered that MSCs interact with T cells and inhibit the proliferation and differentiation of naïve T lymphocytes into Th1 or Th17, increasing the population of natural regulatory T cells (Treg) and enhancing the secretion of anti-inflammatory cytokine, IL-10[67, 68]. Also, MSCs can support expansion and cytotoxicity of cytotoxic T lymphocytes (CTL) that kill cancer cells, damaged cells, or virus-infected cells[69]. MSCs also secrete IL-6 to support allo-stimulated T-cell proliferation and inhibit TNF-α expression by increasing IL-10 expression from stimulated dendritic cells through their expression of IL-1RA[70, 71]. In the pro-inflammatory environment, MSCs secreted anti-inflammatory cytokines, prostaglandin E2 (PGE2), TGF-β1, cyclooxygenase 2, and other factors[72]. Among the anti-inflammatory proteins secreted by MSCs, tumor necrosis factor-α (TNF-α)-inducible gene 6 protein (TSG-6) attenuates inflammatory reactions. TSG-6, an anti-inflammatory protein, suppresses macrophages from expressing inflammatory cytokines in response to mitogen-activated protein kinase (MAPK) signaling[73, 74].

However, the specific mechanisms of the suppression of the inflammatory

reactions from TSG-6 secreted by MSCs, especially dental stem cells, are not well elucidated. In addition, the immune-regulatory role of MSCs has not been clearly explained. Transforming growth factor-β (TGF-β) is not only a critical regulator of osteogenic differentiation by activating downstream Smad signaling pathways[75, 76], but also acts as an immune-regulatory cytokine[47-49]. However, the key mediator involved in both bone formation and inflammation is not well-known.

In the dental research field, PDLSCs, BMSCs, and DFSCs are focused on as important cells that can be utilized to regenerate and repair damaged dental structures[12, 77]. This study analyzes the relationship between bone regeneration and the inflammatory environment of MSCs in damaged dental areas using PDLSCs, BMSCs, and DFSCs. Understanding the role of MSCs on inflammation will help ensure the high-quality bone regeneration. Also, anti-inflammatory cytokines released by MSCs will be tested for their ability to restore bone regeneration capability from an inhibited inflammatory condition.

Therefore, we constructed a local inflammatory environment induced by a high BMP-2 concentration by co-culturing macrophages and MSCs to study the role of MSCs in an inflammatory environment. We hypothesized that a high concentration BMP-2 causes inflammatory reactions of THP-1 cells,

leading to suppression of osteogenesis in MSCs. Also, TSG-6 secreted by MSCs suppressed BMP-2 induced inflammation. This study focused on the interactions of DFSCs with periodontal pathogens to demonstrate the relationship between inflammatory conditions and osteogenesis. The hypothesis is that increased TGF-β2 caused by inflammation prevent the bone formation abilities of DFSCs. These experiments aimed to investigate the influence of human mesenchymal stem cells on inflammation, especially focusing on bone regeneration and anti-inflammatory reactions.

Part I

TSG-6 secreted by mesenchymal stem cells suppresses immune reactions influenced by BMP-2 through p38 and MEK mitogen-activated protein kinase pathway

I. Materials and methods

1. Cell culture conditions

hPDLSCs from impacted third molars of humans (n=8, age 17–29) and BMSCs from human maxilla (n=4, age 20-26) were collected by the Department of Oral and Maxillofacial Surgery at Seoul National University Dental Hospital. This protocol was approved by the Institutional Review Board of the Seoul National University School of Dentistry (IRB No. S-D20080009). Collected PDLSCs and BMSCs were digested separately in 3 mg/ml type 1 collagenase (BioBasic INC., Toronto, ON, Canada) and 4 mg/ml dispase II (Gibco BRL, Long Island, NY, USA) for 1 hour with shaking at 37°C in a 5% CO_2 incubator as previously described[18]. Cultures were in grown in alpha minimum essential medium (α-MEM) supplemented with 100 μM L-ascorbic acid, 2 mM L-glutamine, 100 U/ml antibiotics-antimycotics (all from Gibco), and 15% fetal bovine serum (FBS; Equitech-Bio Inc., Kerrville, TX, USA). PDLSCs and BMSCs from the second to sixth passages were used for experiments. A human monocyte cell line, THP-1, was provided

by the Korean Cell Line Bank (KCLB) and cultured in Roswell Park Memorial Institute (RPMI 1640) supplemented with 100 U/ml antibiotics-antimycotics (both from Gibco) and 10% FBS (Equitech-Bio Inc.).

2. Co-culture of macrophages and mesenchymal stem cells

THP-1 cells were activated with 50 nM phorbol 12-myristate 13-acetate (PMA) for 3 days, followed with 1000 or 5000 ng/ml recombinant human BMP-2 (rhBMP-2; Daewoong Pharmaceutical Co., Seongnam, Korea) for 24 hours. THP-1 cells were stimulated for 3 days in RPMI 1640 medium with PMA, and equal numbers of MSCs were seeded for 1 day and co-cultured in growth medium. MSCs and THP-1 cells were cultured alone as controls. Recombinant human TSG-6 protein (R&D Systems, Minneapolis, MN, USA) were added on THP-1 cells with 10 or 100 ng/ml.

3. Osteogenic differentiation

To induce osteogenic differentiation, MSCs with or without THP-1 cells were cultured in MSC growth medium until 80-90% confluent. Co-cultured cells were changed to differentiation medium consisting of α-MEM supplemented with 10% FBS, 10 nM dexamethasone (Sigma-Aldrich Co., St. Louis, MO, USA), 5 mM glycerol phosphate (Sigma-Aldrich), 100 U/ml

antibiotics-antimycotics (Gibco) and 100 μM L-ascorbic acid. After 5 days of incubation in the osteogenic medium with BMP-2, a QuantiChrom Alkaline Phosphatase (ALP) Assay Kit (BioAssay Systems, Hayward, CA, USA) was used to detect ALP activity following the manufacturer's directions. The absorbance was measured at 405 nm with a microplate reader (Bio-Rad). An alkaline phosphatase staining kit (Sigma-Aldrich) was used to detect alkaline phosphatase in MSCs after 5 days in osteogenic medium. After incubating in differentiation medium for 10 days, BMSCs and PDLSCs were stained with 40 mM alizarin red S solution (pH 4.2) to detect calcium deposits. Stained alizarin red particles were quantified with 20% methanol and 10% acetic acid and detected with a spectrophotometer (Fluostar Optima; BMG LABTECH, Ortenberg, Germany) at 450 nm.

4. RT-PCR & real-time RT-PCR

Total RNA was isolated from cells with an RNA Mini Kit (Ambion, Carlsbad, CA, USA) and reverse-transcribed with a SuperScript III First-Strand Synthesis System kit (Invitrogen, Carlsbad, CA, USA). Reverse transcription polymerase chain reaction (RT-PCR) was performed with the primers listed in Table 1[78]. Real-time RT-PCR was performed on a Real-time PCR System 7500 (Applied Biosystems, Foster City, CA, USA) to quantify

mRNA expression. Glyceraldehyde-3-phosphate dehydrogenase (GAPDH, Hs99999905_m1) was used as an endogenous control. The following human-specific primers and probes (all from Applied Biosystems) were used: TNF-α (Hs01113624_g1), Interleukin (IL)-1β (Hs00174097_m1), and TSG-6 (TNFAIP6; Hs01113602_m1). Expression was quantified by the ΔΔCT method.

5. Flow cytometry analysis.

Activated THP-1 cells were subjected to flow cytometry to detect macrophage phenotypes in the form of CD11b and CD14 expression. Approximately 5 x 10^5 cells were activated with PMA for 3 days, followed with BMP-2 for 24 hours. Activated cells were double-stained with allophycocyanin™7 (APC-7)-conjugated mouse anti-human CD11b (BD Bioscience, Franklin Lakes, NJ, USA*) and* fluorescein isothiocyanate (FITC)-conjugated mouse anti-human CD14 (BD Bioscience). Stained cells were detected and analyzed with a FACS Aria IIII (BD Bioscience).

6. Enzyme-linked immunosorbent assay (ELISA)

To identify cytokines released from THP-1 cells with or without MSCs, the cultured cells were starved in serum-free medium overnight. After overnight

starvation, cells were activated with 1000 and 5000 ng/ml BMP-2 for 24 hours, supernatants containing inflammatory-related products induced by BMP-2 without FBS were collected, and ELISA was performed to determine TNF-α and IL-1β levels. Human TSG-6 ELISA kit was performed for the quantitative measurement of human TSG-6 in supernatants (RayBiotech, Norcross, GA, USA). The absorbance of each sample was measured with a microplate reader (Fluostar Optima, BMG LABTECH) at 450 nm.

7. Immunocytochemistry

A total of 10^5 THP-1 cells were plated and cultured in 2-well chamber slides with 50 nM PMA in RPMI 1640 medium for 3 days. Stimulated THP-1 cells were incubated without FBS overnight. Starved THP-1 cells were treated with 5000 ng/ml BMP-2 and 10 - 100 ng/ml TSG-6 for 3 hours. After fixation, blocked cells were incubated with anti-NF-kB p65 antibody (Abcam, Cambridge, UK) in blocking solution at 4°C overnight. The cells were then incubated in anti-rabbit IgG secondary antibody (Abcam) for 1 hour. Mounting medium with DAPI (Vector Laboratories, Burlingame, CA, USA) was used to stain nuclei. Fluorescent imaging was performed on a confocal laser scanning microscope (FV300, Olympus America Inc., Center Valley, PA, USA).

8. Western blotting analysis

PMA-stimulated THP-1 cells were cultured and treated with 5,000 ng/ml BMP-2 and 10 ng/ml TSG-6 for 10, 30, or 60 minutes. Proteins from THP-1 cells were collected with cell extraction buffer (Invitrogen) with protease inhibitors and 1 mM phenylmethane sulfonyl fluoride. Proteins on membranes were detected with p-NF-κB, NF-κB, p-Erk1/2, Erk1/2, p-JNK, JNK, p-p38, and p38 primary antibodies (1:1000, Cell Signaling Technologies, Boston, MA, USA) followed by HRP-linked secondary antibody. As a control, β-actin (1:1000) antibody was used. The immunoblots were visualized with an HRP chemiluminescent detection kit (SurModics, Eden Prairie, MN, USA) and measured with the MicroChemi analyzer (DNR Bio-image Analyzer).

9. Immunohistochemistry

Collagen-sponges under 1 cm were transplanted and isolated after 24 hours. Collected scaffold and surrounded tissues were blocked and sectioned for H&E staining and immunohistochemistry. To detect infiltrated activated macrophages, F4/80 antibody (Abcam 100790, 1:100) were used.

10. Antibody array

For the semi-quantitative detection of 40 human inflammatory related proteins, antibody array (RayBiotech, Inc., Norcross, GA, USA) were used. Supernatants from 24 hours incubation with BMP-2 were selected to detect the cytokines. The immunoblots were visualized with an HRP chemiluminescent detection and measured with the MicroChemi analyzer (DNR Bio-image Analyzer).

11. Statistical analysis

Statistical analysis was performed with one-way ANOVA followed by Tukey's HSD test with SPSS 22 (SPSS Inc., Chicago, IL, USA). ELISA data are presented as the mean ± SE from quadruple replicates and others from triplicate replicates. Statistically significant difference between data was assigned if $p < 0.05$.

II. Results

1. The involvement of macrophages in BMP-2 induced inflammation.

Dense infiltration of inflammatory cells was observed around the grafted collagen sponge with 20 μg/ml of BMP-2 on the dorsal side of mouse (Fig. 1a,b). Immunohistochemical staining for macrophages were performed and added the results to Fig. 1c. Infiltrated macrophages were stained with F4/80, a macrophage marker (Fig. 1c). Infiltrated macrophages were detected and stained with F4/80 antibody around grafted collagen sponges with 10 μg/ml and 20 μg/ml BMP-2.

2. High concentrations of BMP-2 inhibit early osteogenic differentiation of mesenchymal stem cells

In the early stages of osteogenic differentiation, hPDLSCs and hBMSCs had low levels of ALPase activity in the presence of 1,000 or 5,000 ng/ml BMP-2

on day 5 (Fig. 2a). This pattern was identical to that of ALP staining (Fig. 2b). Both BMP-2 concentrations suppressed early osteogenic differentiation in hPDLSCs and hBMSCs. However, hMSCs co-cultured with THP-1 cells had higher levels of ALPase activity in the early stages than did hMSCs alone.

3. Co-culturing mesenchymal stem cells with THP-1 cells inhibits late osteogenic differentiation

The late stages of osteogenic differentiation were evaluated by alizarin red S staining (Fig. 3a, b). The inhibitory effect of THP-1 cells on osteogenic differentiation was overcome by BMP-2 in the late stages of differentiation. However, co-cultured hMSCs and THP-1 cells underwent less osteogenic differentiation in the late stages than did MSCs alone. Consequently, the initially inhibitory effect of BMP-2 concentrations changed to an inductive osteogenic signal in the late stages.

4. Characteristics of THP-1 cells in BMP-2-induced inflammation

THP-1 cells did not attach to the culture dish without PMA treatment. BMP-2 alone cannot induce morphological changes implying the activation of THP-1 cells. Therefore, experiments were performed after PMA activation (Fig. 4).

To determine the response to BMP-2 of each cell, the gene expression of BMP-related receptors on THP-1 cells, PDLSCs, and BMSCs was determined by RT-PCR. The BMP receptors related to signaling consist of the type I receptors ALK2, ALK3, and ALK6 and the type II receptors Act-RIIA, Act-RIIB, and BMP-RII. The gene expression of BMP-related receptors differed among THP-1 cells, PDLSCs, and BMSCs (Fig. 5a). The activation of THP-1 cells was examined via flow cytometry analysis. CD11b and CD14 expressed on activated macrophages from monocytes were double-stained to examine the activation of THP-1 cells. In the absence of stimulation by PMA, THP-1 cells were not activated (Fig. 5b). Surface expression of activated macrophage markers, CD14 and CD68, on activated THP-1 cells changed in response to BMP-2 treatment. CD14 and CD68 were overexpressed at 5,000 ng/ml BMP-2. BMP-2 at a concentration of 5000 ng/ml also activated the inflammatory stage of THP-1 cells (Fig. 5c). As shown in Fig. 3d, 5000 ng/ml BMP-2 induced an inflammatory response in THP-1 cells. THP-1 cells highly expressed TNF-α and IL-1β in the presence of 5,000 ng/ml BMP-2.

5. Mesenchymal stem cells inhibit inflammatory cytokine expression in THP-1 cells

To identify the other anti-inflammatory factors, IL-1 receptor antagonist,

prostaglandin E2, and IL-10, among others, on MSCs, we tested an antibody array for anti-inflammatory cytokines IL-10 and TGF-β1 released from MSCs on BMP-2 treatment (Fig. 6). However, there were no significant changes in the expression of IL-10 and TGF-β1.

To examine the immunosuppressive effects of hMSCs on BMP-2-induced inflammation, pro-inflammatory gene expression and protein accumulation in response to BMP-2 treatment were determined by real-time RT-PCR (Fig. 7b, c) and ELISA (Fig. 7d, e) following the experimental scheme (Fig. 7a). With 24-hour BMP-2 treatment, 5,000 ng/ml BMP-2 was required for PMA-stimulated THP-1 cells to release pro-inflammatory cytokines. Stimulated THP-1 cells increased expression of the TNF-α and IL-1β genes in the presence of 5,000 ng/ml BMP-2. Co-culturing THP-1 cells in the presence of PDLSCs or BMSCs decreased levels of inflammatory cytokines IL-1β and TNF-α. PDLSCs significantly suppressed the gene expression of inflammatory cytokine IL-1β more than BMSCs did. The suppression of TNF-α genes in co-culturing THP-1 cells with PDLSCs was similar to the suppression in BMSCs (Fig. 7b, c). The levels of TNF-α and IL-1β proteins followed a pattern similar to gene expression in response to BMP-2 treatment (Fig. 7d, e). This result demonstrated that PMA-stimulated THP-1 cells secreted excessive levels of inflammatory cytokines in the presence of 5,000

ng/ml BMP-2, thereby worsening the local inflammatory environment. In contrast, TNF-α and IL-1β expression induced by PMA was significantly suppressed by co-culture with MSCs.

6. TSG-6 secreted by mesenchymal stem cells in response to BMP-2 interferes with inflammatory reactions of THP-1 cells through MAPK signaling

In the presence of 5,000 ng/ml BMP-2, both PDLSCs and BMSCs secreted a significant amount of TSG-6 as shown by real-time RT-PCR (Fig. 8a). PDLSCs and BMSCs treated with 5000 ng/ml of BMP-2 secreted significant protein levels of TSG-6 (Fig. 8b). Also, PDLSCs and BMSCs co-cultured with THP-1 cells in 5000 ng/ml BMP-2 also showed increased protein expression of TSG-6. TSG-6 lowered IL-1β expression by BMP-2-treated THP-1 cells. Moreover, a BMP-2 concentration of 5,000 ng/ml increased IL-1β expression, which was significantly inhibited by exogenous TSG-6 (Fig. 8c, d). TNF-α expression did not change in response to TSG-6 induced by 5000 ng/ml BMP-2 (data not shown). Treatment with 100 ng/ml TSG-6 for 3 hours with BMP-2 induction blocked NF-κB translocation to the nucleus in THP-1 cells (Fig. 8e). Western blotting revealed that TSG-6 blocked NF-κB phosphorylation (Fig. 8f).

The effect of TSG-6 on downstream NF-κB signaling in THP-1 cells showed that ERK1/2 (Fig. 9a) and p38 signaling (Fig. 9b) were blocked at 60 min, whereas TSG-6 did not affect JNK signaling during BMP-2 treatment (Fig. 9c). Moreover, TSG-6 treatment for 60 min inhibited JNK signaling. This result indicates that TSG-6 secreted by MSCs blocks NF-κB translocation and IL-1β secretion through NF-κB/Erk1/2/p-38 signaling in THP-1 cells.

III. Discussion

This study was designed to investigate the immunosuppressive effects of MSCs on immune reactions triggered by macrophages at high BMP-2 concentrations. In current clinical and experimental applications of BMP-2, the inflammatory response induced by high concentrations of exogenous BMP-2 may decrease initial bone formation. Our study suggests that high BMP-2 concentrations boost the initial local inflammatory reaction by releasing inflammatory cytokines, while MSCs reduce the inflammatory reaction through TSG-6.

Bone remodeling/regeneration is a consequence of the balancing mechanism between osteoblasts and osteoclasts[79, 80]. Monocytic macrophages were selected as candidate immune cells in this study because they are derived from a hematopoietic lineage related to osteoclasts. Monocytes from blood vessels

differentiate and activate into macrophages after infiltrating blood vessels in inflammatory sites, and can then differentiate into osteoclasts[81, 82]. Similarly, we observed that high doses of BMP-2 triggered the infiltration and activation of macrophages. Our *in vitro* experimental scheme mimicked the *in vivo* clinical applications. Previous studies on BMP-2-related swelling indicated the involvement of immune cells, such as monocytes, macrophages, and lymphocytes[41, 42]. Also, macrophages co-cultured with MSCs have been studied. In tissue repair, MSC-co-cultured macrophages showed high phagocytic activity and infiltration in wound sites[63, 83].

Another reason for focusing only on macrophages among immune cells is the osteoclastic activity of monocyte/macrophages. There were also practical reasons for choosing macrophages; we performed *in vitro* experiments to verify immune cell reactions, and macrophages are affordable to co-culture. Although PMA treatment on THP-1 cells was prerequisit to differentiate dormant THP-1 cell into stimulated macrophage which can attach to culture dish and secret inflammatory cytokines, we were able to test the interaction between MSCs and PMA-activated macrophages in the presence of BMP-2. In our research, a monocytic macrophage cell line, THP-1, was activated with PMA for conversion to convert them into activated inflammatory cells. At the same time, osteogenic medium was applied to MSCs to drive differentiation

into osteoblasts or THP-1 cells. A previous study showed that BMP-2 secretion was increased in co-cultured MSCs and monocytes/macrophages in the early stages of osteogenic differentiation[84]. Alkaline phosphatase (ALP) is an early osteogenic marker; however, some researchers have also found ALP to be an indicator of inflammation. ALP was induced during acute and chronic inflammation in rodent and human models[85, 86]. In this experiment, THP-1 cells were influenced by an inflammatory condition, PMA activation, which may affect early ALP activity. Our co-cultured MSCs and macrophages exhibited enhanced early osteogenic differentiation (ALPase activity) relative to MSCs alone. However, a high concentration of exogenous BMP-2 inhibited the early stages of osteogenesis in both MSCs alone and MSCs co-cultured with THP-1 cells. Previous studies demonstrated that the inflammatory environment inhibits osteoblastic differentiation[2]. In the present study, alizarin red S staining indicated that the late stages of osteogenic differentiation were suppressed in MSCs co-cultured with macrophages. In addition, osteogenic differentiation induced by high BMP-2 concentrations was reversed, resulting in higher calcium deposits in the late stages of osteogenesis. This reversal in the late stages of osteogenic induction may be explained by discontinued PMA treatment of THP-1 cells. Therefore, the effects of inflammatory macrophages were reduced in late osteogenesis in our experiments. Reduced

inflammatory effects increased the osteogenesis of hMSCs. This can explain the contrasting effects on BMP-2 on the early and late stages of osteogenesis.

Clinical disorders of osteoporosis involving inflammatory conditions include rheumatoid arthritis, cystic fibrosis, and periodontitis[3, 87]. Our results indicate that an inappropriately high BMP-2 concentration stimulates macrophages to secrete inflammatory cytokines and delay osteogenic differentiation in MSCs. This implies that the reduced bone formation seen in clinical use of high BMP-2 concentrations is caused by increased inflammatory cytokines. BMP-2 is thought to be responsible for inducing a pro-inflammatory environment. The inflammatory characteristics of rhBMP-2 have been observed *in vitro* and *in vivo* in the form of soft tissue swelling and inflammatory cytokine release in a rodent model[88, 89]. We also found that monocytic macrophages express the genes for type I and type II BMP receptors. PDLSCs and BMSCs also express BMP receptors at differing levels, suggesting that BMP-2 affects downstream signaling heterogeneously in immune cells and MSCs. Our results show that BMP-2-induced macrophages caused the secretion of several inflammatory cytokines. In MSCs, however, BMP-2 participated in both Sma- and Mad-related family (SMAD) and MAPK signaling to increase the expression of osteogenic-related genes. In BMP-2-induced inflammation, MSCs differentiated into osteoblasts to a lesser degree, supporting previous studies

that TNF-α and IL-1β can inhibit MAPK signaling to reduce osteogenic gene expression in murine MSCs[42, 90].

According to other articles, TSG-6 affects macrophages as an anti-inflammatory factor[91, 92]. Other anti-inflammatory factors on MSCs did not influence macrophages [51]. In a BMP-2 transplantation rodent model, infiltration of mononuclear cells in between transplanted collagen and tissue fibers is more common than other immune cells[32, 44]. In our scheme, we focused on the relationships between macrophages and MSCs. This suggested that macrophages could effectively show to show the immunosuppressive effects of TSG-6 secreted by hMSCs. Further studies on TSG-6 will be performed with future *in vivo* transplantation.

In addition to osteoblast differentiation, another MSC function is immunomodulation[51, 93, 94]. In disease models, MSCs suppress inflammatory responses through several mechanisms[74, 95-98]. Our results suggested that MSCs secrete TSG-6 in response to BMP-2. This result indicates that administering a high BMP-2 concentration to MSCs triggers an anti-inflammatory reaction that affects macrophages. In MSC and macrophage co-cultures, inhibited macrophage secretion of inflammatory cytokines, such as IL-1β and TNF-α was observed. PDLSCs suppressed inflammation more effectively at a higher BMP-2 concentration than did BMSCs. The results

showed less IL-1β upon treating macrophages with TSG-6, which was consistent with macrophage and MSC co-cultures. Previous studies showed that TSG-6 from MSCs regulates macrophages through NF-κB signaling triggered by lipopolysaccharide (LPS) or zymosan-induction[90, 92, 99]. At a high BMP-2 concentration, macrophages induced NF-κB translocation into the nucleus, similar to that seen in LPS- or zymosan-induced inflammation. With TSG-6 treatment, NF-κB phosphorylation was inhibited in THP-1 cells at a high BMP-2 concentration. Although studies have tested the inhibition of inflammation by TSG-6, there is little agreement regarding how inflammatory cytokines and osteogenic stimulation are differentially activated during NF-κB signaling in MSCs[74, 90, 100].

In conclusion, the release of inflammatory cytokines by PMA-activated macrophages was increased by a high BMP-2 concentration. TSG-6 secreted by MSCs suppressed inflammatory reactions related to high BMP-2 concentrations through MAPK signaling in macrophages. The differing tendencies of PDLSCs and BMSCs in the presence of BMP-2 should be studied in the context of oral maxillofacial reconstruction therapy. By determining the anti-inflammatory effects of TSG-6 from dental tissue-derived MSCs, we can expand the use of MSCs in clinical trials, especially in bone-related diseases, by establishing optimal therapeutic BMP-2

concentrations.

Part II

TGF-β2 downregulates bone formation in inflammatory condition

I. Materials and methods

1. Primary cell culture

Human normal (n=6, male/female, age 15-21) and inflamed primary dental follicles (n=1, female, age 18) were collected by the Department of Oral and Maxillofacial Surgery at Seoul National University Dental Hospital. This protocol was performed under an approved protocol by the Institutional Review Board of the Seoul National University School of Dentistry (IRB No. S-D20080009). Cell isolation was based on previous reports with modifications[18]. Collected dental follicle stem cells (DFSC) was incubated at 37°C for 1 hour for digestion in 3mg/ml type 1 collagenase (BioBasic INC., Toronto, ON, Canada) and 4 mg/ml dispase II (Gibco-BRL, Waltham, MA,

USA) for 1 hour. Isolated mesenchymal stem cells were cultured in alpha minimum essential medium (α-MEM; Gibco-BRL) containing L-ascorbic acid (100 μM, BioBasic INC.), L-glutamine (2 mM, Gibco-BRL), penicillin (100 units/ml, Gibco-BRL), streptomycin (100 μg/ml, Gibco-BRL), amphotericin B (0.25 μg/ml, Gibco-BRL), and 15% fetal bovine serum (FBS; Equitech-Bio Inc., Kerrville, TX, USA). The cells were incubated at 37°C in a humidified 5% CO_2 and medium was changed every 2-3 days. Dental follicle stem cells at early passages (1-6) were used in this experiments.

2. Proliferation and cell viability assay

Normal and inflamed DFSCs of each passage was incubated for 3 days. For colony forming assay, 500 cells were seeded and fixed with 4% formaldehyde (Sigma-Aldrich Co.) after 10 day incubation, and stained with 1% crystal violet (Sigma-Aldrich Co.). Colonies, consisted of more than 50 cells, were counted at passage 2 and 4. Colony forming efficiency was calculated as a percentage of the number of seeded cells. To measure the cumulative population doubling, normal and inflamed dental follicle stem cell was counted at day 3, 6, 9, 13, 16, and 19. Cell viability was performed by 3-(4,5-dimethylthiazol-2-yl)-2,5-diphenyltetrazolium bromide (MTT) assay. The optical density of formazan crystals dissolved in DMSO was read at 540 nm. Normal DFSCs were treated with 10 ng/ml of TGF-β2 (R&D systems). After

1, 2, and 3 days, DFSCs were counted and assayed with MTT solution.

3. Nitric oxide (NO) assay

To mimic the inflammatory environment on dental follicle tissue, DFSCs were seeded and cultured with *Porphyromonas gingivalis* (P.g) LPS (055:B5, Sigma-Aldrich Co., St. Louis, MO, USA). Supernatants were collected after 24 hours and 48 hours incubation at 10, 100 and 1000 ng/ml concentration of LPS. Nitric oxide production levels were done by Quantichrom NO assay kit (BioAssay Systems) following the manufacturer's manuals. The absorbance was read at 540 nm.

4. RT-PCR & real-time PCR

Collected total RNAs with RNA mini kit (Ambion, Carlsbad, CA, USA) were reverse-transcribed to complementary DNA using SuperScript III First-Strand Synthesis Systems kit (Invitrogen, Carlsbad, CA, USA). Real-time PCR System 7500 (Applied Biosystems, Foster City, CA, USA) measured mRNA expression using primers and probes; Glyceraldehyde-3-phosphate dehydrogenase (GAPDH, Hs99999905_m1) as an endogenous control, TNF-α (Hs01113624_g1), IL-6 (Hs00985639_m1), IL-8 (Hs00174103_m1),

osteocalcin (Hs01587814_g1), ALP (Hs01029144_m1), and type I collagen (Hs00164004_m1). mRNA expression was examined with primers; IL-1β (forward, 5'-TCATTGCTCAAGTGTCTGAAGC-3'; reverse, 5'-TGGTCGGAGATTCGTAGC-3'), IL-8 (forward, 5'-ACTGAGAGTGATTGAGAGTGGAC-3'; reverse, 5'-AACCCTCTGCACCCAGTTTTC-3') and IL-6 (forward, 5'-GAA AGCAGCAAAGAGGCACT-3'; reverse, 5'-TTTCACCAGGCAAGTCTCCT-3'), stathmin (forward, 5'-ACTGCCTGTCGCTTGTCT; reverse, 5'-GTCTCGTCAGCAGGGTCT-3'), spondin-2 (forward, 5'-CGGCCAAATACAGCATCACC-3'; reverse, 5'-CCCAGCAGCGAAGACCACT-3'), layilin (forward, 5'-AGGAGTAAGGAGTCTGGATGGGTG-3'; reverse, 5'-GGATGACTGGCTGGGATAAAGGA-3'), TGF-β1 (forward, 5'-GGACACCAACTATTGCTTCAG-3'; reverse, 5'-TCCAGGCTCCAAATGTAGG-3'), TGF-β2 (forward, 5'-GGCTCAGTGGGCAGCTTGT-3'; reverse, 5'-GCTCAATCCGTTGTTCAGGC-3'), and GAPDH (forward, 5'-AGCCGCATCTTCTTTTGCGTC-3'; reverse, 5'-TCATATTTGGCAGGTTTTTCT-3').

5. ELISA

Supernatants from DFSCs treated with 10, 100, 1000 ng/ml concentrations of LPS for 24 and 48 hours were collected to analyze the levels of IL-6 and IL-8 at 10, 100 and 1000 ng/ml LPS concentrations. Human IL-6 and IL-8 were measured by Quantikine ELISA kits (RnDSystems, Minneapolis, MN, USA). The absorbance was read at 450 nm.

6. Protein profile analysis & Mass Spectrometry analysis

Normal and inflamed DFSCs were cultured for 24 hours to collect the supernatant. Proteins from each cell culture media was purified and concentrated by centrifugal filter devices (Merck, Billerica, MA, USA). Concentrated 25 μg of proteins were analyzed and compared using 12% Sodium dodecyl-polyacylamide gel electrophoresis (SDS-PAGE) stained with coomassie brilliant blue (CBB). Selected bands from 1-dimensional gel electrophoresis (1-DE) were digested by trypsin and analyzed by liquid chromatography coupled with tandem mass spectrometry (LC-MS/MS). All tandem mass spectra were searched against the NCBI database with the Mascot search engine (Matrix Science, London, U.K.). Peptides were identified with a Mascot score of 30 or above.

7. Osteogenic differentiation

A. *In vitro* osteogenic differentiation

At 40-50 % confluent, culture medium were replaced with α-MEM containing dexamethasone (10 nM, Sigma-Aldrich Co., St. Louis, MO, USA), glycerol phosphate (5 mM, Sigma-Aldrich), penicillin (100 units/ml, Gibco-BRL), streptomycin (100 μg/ml, Gibco-BRL), amphotericin B (0.25 μg/ml, Gibco-BRL), and L-ascorbic acid (100 μM, BioBasic INC.) and 10% FBS (Equitech-Bio Inc.) for osteogenic differentiation with or without 100 ng/ml LPS and TGF-β2 inhibitor (R&D systems, Minneapolis, MN, USA). At day 7, alkaline phosphatase (ALP) activity was measured by using a QuantiChrom assay kit (BioAssay Systems, Hayward, CA, USA) following the manufacturer's manuals. With 14-28 days induction, cells were stained with 40 mM alizarin red S solution (pH 4.2, Sigma-Aldrich) for 15 minutes to visualize the calcium accumulation in mineralized cells. Quantification of alizarin red S was done by destaining with a solution of 20% methanol and 10% acetic acid. Optical density of dissolved solvent was read at an absorbance of 450 nm.

B. *In vivo* transplantation & Immunohistochemistry

The care, maintenance, and treatment of animals in these experiments followed protocols approved by the Institutional Animal Care Committee of Seoul National University (SNU-140501-9-1). About 5 x 10^6 Normal and inflamed DFSC were implanted into the dorsal surface of immunocompromised nude mice (NIH-bg-nu-xid, Harlan Sprague Dawley, Indianapolis, IN, USA) with 40 mg of hydroxyapatite/tricalcium phosphate particles (HA/TCP, Zimmer, Warsaw, IN, USA). The transplants were harvested and fixed with 4% paraformaldehyde. Fixed transplants were decalcified with 10% EDTA (pH 8.0, Sigma-Aldrich) and embedded in paraffin. Hematoxylin and eosin (H&E) staining was performed on tissue sections. For immunohistochemistry (IHC) staining, mouse anti-human mitochondria antibody (1:200, Chemicon, Temecula, CA), mouse anti-human osteocalcin antibody (1:100, Abcam, Cambridge, UK) and rabbit anti-human collagen type 1 (1:800, Abcam) were used by following anti-mouse/rabbit HRP/DAB detection kit (Abcam).

8. Western Blot

DFSCs were seeded onto 6-well plates at 2 x 10^5 cells per well. After

overnight starvation, the cells were treated with 0.1 μg/ml LPS for 30 minutes with or without 0.5 and 1 μg/ml TGF-β2 inhibitor (R&D systems). Cell extracts were collected with lysis buffer (Invitrogen) containing protease inhibitors and 1 mM phenylmethanesulfonyl fluoride. Proteins collected from each sample were separated and transferred to PVDF membrane, detecting with p-smad 2/3, smad 2/3, RUNX2, β-actin antibody (1:1000; Cell Signaling Technologies, Boston, MA, USA) followed by HRP-linked secondary antibody (1:1000). The immunoblots were detected by an HRP chemiluminescent detection kit (SurModics, Eden Prairie, MN, USA) and measured with the MicroChemi analyzer (DNR Bio-image Analyzer).

9. Statistical analysis

Data are presented as **mean ± SE** from at least in triplicate. Statistically significant differences between groups were performed with Student's t-test and one-way ANOVA followed by Tukey's HSD test with SPSS 22 (SPSS Inc., Chicago, IL, USA). $P < 0.05$ was considered statistically significant.

II. Results

1. Proliferation and osteogenic differentiation of normal and inflamed dental follicle stem cells

Isolated DFSCs from normal and inflamed dental follicle tissues were cultured in stem cell growth medium. As shown in Figure 10a and 1a, CFE from inflamed DFSCs (7.8 ± 1.9%) was significantly higher ($p < 0.05$) compared to normal DFSCs (14.7 ± 0.81%) at passage 2. Similar to passage 2, the CFE from inflamed DFSCs was also higher compared to normal DFSCs at passage 4. DFSCs from each groups were expanded over passage 9 with similar growth kinetics. An appreciable increase in the number of population

doubling of inflamed DFSCs was observed after passage 13, indicating that the proliferative potential of inflamed DFSCs was higher than those of normal DFSCs (Fig. 10c). Inflamed DFSCs had higher proliferation potentials compared to normal DFSCs.

For the evaluation of the inflammation on the osteogenic differentiation of normal and inflamed DFSCs the alizarin red (Fig. 10d, e) and ALP activity (Fig. 10f) were estimated.

ALP activity, as an early marker of osteogenic differentiation, were assessed at day 7. ALP activity of normal DFSCs was significantly increased about 2.5 fold compared to that of inflamed DFSCs. Similarly, calcium deposits of normal DFSCs were highly observed compared to those of inflamed DFSCs. Inflamed DFSC showed about 5 fold lower amounts of calcium deposits from quantification of mineral contents than normal DFSCs. The osteocalcin expression was significantly lower in the inflamed DFSCs than in the normal DFSCs (Fig. 10g). However, ALP and type 1 collagen was not significant at mRNA levels. From osteogenic differentiation on normal and inflamed DFSCs, there were significant differences.

2. *In vivo* transplantation of normal and inflamed dental

follicle stem cells

The decreased patterns of osteogenesis on *in vitro* were also similar to hard tissue formation on *in vivo* transplantation of DFSCs on the backside of nude mice with HA-TCP carriers for 8 weeks. Dental pulp stem cells (DPSCs) were used as positive control. With comparison of hard tissue formation in H&E staining, transplants with inflamed DFSCs showed less hard tissue formation than that of normal DFSCs (Fig. 11a). Immunohistochemistry was done to confirm the transplanted human DFSCs by using human mitochondria antibody (Fig. 11b). Hard tissue were positively stained with osteocalcin and type 1 collagen antibodies (Fig. 11c,d) These results indicated that hard tissue were formed by human normal and inflamed DFSCs. Both *in vitro* and *in vivo* transplantation results showed that inflamed DFSCs showed lower levels of osteogenic differentiation.

3. Protein identifications from normal and inflamed dental follicles stem cells

RT-PCR was conducted to assess higher expression of pro-inflammatory cytokines, such as IL-6, IL-8, and IL-1β on inflamed DFSCs (Fig. 12a). To evaluate the differences between normal and inflamed DFSCs, protein profile

analysis was done followed by LC-MS/MS. Purified and extracted proteins of each cell were harvested by centrifugation and separated using 1-dimensional SDS-PAGE (Fig. 12b). A considerably different concentration of protein was found in inflamed DF and normal DF sample, particularly at molecular weights of about 15, 17, 25, 30, and 50 kDa. These bands were identified with LC-MS/MS and analyzed with Mascot engines (Table 2). Among proteins with above Mascot score of 30, proteins related to osteogenesis, proliferation, and inflammation were selected. Between normal and inflamed DFSCs, stathimin, spondin-2, and layilin genes were enhanced at inflamed DFSCs in normal condition (Fig. 12c). Whereas TGF-β1 gene from normal and inflamed DFSCs didn't change in normal growth condition, TGF- β2 from inflamed DFSCs was slightly increased than that from normal DFSCs. On the other hand, the osteogenic condition influenced differently on the expressions of TGF-β1 and TGF-β2. TGF-β2 gene of inflamed DFSCs were significantly increased in osteogenic condition. From protein profiling analysis and RT-PCR, inflamed DFSCs during osteogenic differentiation showed increased TGF-β2 gene expressions (Table 2, Fig. 12c).

4. Inflammatory environments mimicked by P.g-derived

LPS on DFSCs

To mimicking the inflammatory environment, LPS treatment were used. While treating P.g-derived LPS on normal DFSCs for 24 and 48 hours, the concentrations of nitric oxide (NO) from supernatants were increased in response to 10, 100, 1000 ng/ml LPS (Fig. 13a). LPS-stimulated NO productions of DFSCs were significantly increased at 100 and 1000 ng/ml LPS. To verify whether *P.g.*-derived LPS promoted the inflammatory environment, pro-inflammatory cytokines IL-6 and IL-8 expressions were determined by RT-PCR (Fig. 13b). Results indicated that 1000 ng/ml of LPS provoked both IL-6 and IL-8 genes during 48-hour treatment. Also, there were slight decline on TGF-β1 gene on 48 hours LPS treatment. However, TGF-β2 didn't change the expression on normal conditional medium with LPS treatment. ELISA results also confirmed that LPS treatment mimicked the inflammatory environment on DFSCs by secretion of IL-6 (Fig. 13c) and IL-8 (Fig. 13d). These results has shown that *P.g.*-derived LPS constructed the inflammatory condition on DFSCs like inflamed DFSCs.

5. Influences of LPS on proliferation and osteogenic differentiation of DFSCs

To determine the inflammatory effects on proliferation and osteogenesis, DFSCs were stimulated with LPS during osteogenesis. Concentration 100 ng/ml of LPS didn't affect the cell viability (Fig. 14a). However, the pro-inflammatory cytokines, IL-6 and IL-8, were secreted from DFSCs with significant difference in normal condition (Fig. 14b). These secretion of inflammatory cytokines were maintained during osteogenesis (Fig. 14c). In early stage of osteogenesis, IL-6 and IL-8 were expressed on osteogenic differentiation. Also, the inflammatory environment triggered by LPS on DFSCs provokes the suppression of calcium deposit formation (Fig. 14d, e). Similar to alizarin red s staining, osteocalcin expression on LPS treatment were significantly decreased about 55 fold compared to control with no LPS treatment (Fig. 14f). Interestingly, TGF-β1 gene were highly expressed during osteogenesis, on the contrary, the amount of TGF-β1 were suppressed on LPS-treated osteogenic differentiation. Also, TGF-β2 in osteogenic differentiation were decreased, while LPS treatment in osteogenic differentiation triggered the expression of TGF-β2 on DFSCs (Fig. 14g). These overall results demonstrated that LPS treatment mimicked the inflammatory environment on DFSCs, similar to inflamed DFSCs.

6. The effects of TGF-β2 on LPS-stimulated osteogenic differentiation

To demonstrate that TGF-β2 exerts a strong influence on osteogenic differentiation, TGF-β2 inhibitors were used to prevent the down-mechanisms of TGF-β2 on inflammatory environments. By inhibiting TGF-β2 mechanisms, DFSCs have possibility to differentiate into osteogenic tissues. According to alizarin red S staining (Fig. 15A, B), LPS treatment suppressed the osteogenic differentiation, while TGF-β2 inhibitors overcome the down-regulation of osteogenic differentiation. With 0.5 and 1 μg/ml of TGF-β2 inhibitors, ALP activity of DFSCs was increased by suppressing TGF-β2 regulation (Fig. 15c). These results showed calcium deposits from DFSCs have increased from inhibition of TGF-β2.

While suppressing the osteogenic differentiation by LPS, TGF-β2 inhibitors overcome the suppression of osteogenesis in the concentrations of 0.5 and 1 μg/ml of TGF-β2. Gene expressions of type I collagen (ColI) and osteocalcin (OCN) showed similar patterns with ALP activity and alizarin red S staining (Fig. 15d). With treating the inhibitors of 0.5 and 1 μg/ml TGF-β2, down-regulated gene expression of OCN were increased. However, both ColI and OCN genes didn't change the expression with 0.5 and 1 μg/ml TGF-β2

inhibitors treatment. Also, TGF-β1 gene didn't change with treatment of TGF-β2 inhibitors. Interestingly, IL-8 and IL-6 genes were increased with LPS and decreased with TGF-β2 inhibitors. Also, smad2/3 of DFSCs have phosphorylated with LPS treatment in time-dependent manners. After 30 minutes of LPS treatment on DFSCs, smad2/3 signaling was triggered (Fig. 15e). With TGF-β2 inhibitors and osteogenic differentiation, Runx2 expression was increased compared to low levels of RUNX2 on TGF-β2 inhibitors only (Fig. 15f). To demonstrate the effects of TGF-β2 on DFSCs without immune environment, 10 ng/ml of TGF-β2 were treated. The cell counting and MTT assay results supported slightly increase of proliferation on DFSCs at day 1, 2, and 3 (Fig. 16a,b). Also, ALP activity and alizarin red S staining indicated that TGF-β2 inhibited the osteogenic differentiation (Fig. 16c-e). These overall data indicated that LPS-treated DFSCs have suppressed the osteogenic differentiation and increased TGF-β2.

III. Discussion

Dental follicle tissue is easily obtained from developing teeth especially wisdom teeth during third molar extraction in adolescent patients. Dental follicle stem cells (DFSCs) are known for a candidate to regenerate the dental tissue destructed by oral diseases. With several pathogens, the development of dental stem cells were inhibited, thus bone formation were suppressed. Even though LPS-induced inflammation occurs the aberrant low levels of bone formation, the interactions between inflammation and bone formation on MSCs were still unclear. In this study, we demonstrated that TGF-β2 triggered

by inflammation mediate the inhibition of osteogenic differentiation.

Comparison between DFSCs in normal and inflamed tissues showed different proliferation and osteogenic differentiation. Interestingly, inflamed DFSCs have higher proliferative efficiency from CFU forming assay and calculation of population doubling. However, high proliferative inflamed DFSCs have shown low levels of osteogenic differentiation. The gene expression of osteocalcin was decreased significantly on inflamed DFSCs. Also, ALPase activity showed that inflamed DFSCs suppressed early stage of osteogenic differentiation. The results from *in vivo* transplantation indicate that normal DFSCs show high levels of bone formation than that of inflamed DFSCs. Our results show the similarity to the results of suppressive bone formation on osteoporosis and periodontitis model[101, 102]. Animal models connected to inflammation prove that inflammatory cytokines can inhibit the cell differentiation. However, it has not proved that underlying mechanisms interact between inflammatory cytokine and osteogenic differentiation.

To clarify the differences between normal and inflamed DFSCs, the proteins from each sample were analyzed with LC-MS/MS. The analysis indicated that TGF-β1 and TGF-β2 protein levels in normal and inflamed DFSCs were inversely expressed during osteogenic differentiation. Especially, inflamed DFSCs expressed significantly higher TGF-β2 gene than normal DFSCs.

BMP-2, a member of TGF-β superfamily, was well-known for involving in regeneration of bone. TGF-β1 was also famous for anti-inflammatory cytokines to inhibit the immune cells; T cells, B cells, NK cells, and macrophages[48, 103]. Intriguingly, TGF-β1 secreted by MSCs is important to mediate T cell inhibition. However, unlike well studied anti-inflammatory regulator, TGF-β1, the role TGF-β2 gene expression in inflammation, especially accompanying osteogenesis, was not well reported. Few studied about interactions of inflammation with TGF-β has been done with treatment of TGF-β1 and TGF-β2 to mouse MSCs[103]. While triggering the immune reaction with IFN-γ and TNF-α, mouse MSCs decreased iNOS expression, as a marker of inflammation, in dose-dependent manner with TGF-β1. On the contrary, iNOS expression was down-regulated with TGF-β2 treatment. It coincides well with our results about higher expression of TGF-β2 of inflamed DFSCs.

In a similar fashion to inflamed tissue, LPS was treated to DFSCs to mimic the local inflammatory environment. In the present study, LPS is a key factor to regulate the inflammatory response and differentiation of MSCs. Some reports suggested that LPS inhibited osteogenic differentiation on different MSCs with MAPK signaling[57, 60]. Unlike other oral derived stem cells, DFSCs were only stimulated with LPS from Escherichia coli[13]. In our study, with 48

hours LPS treatment, nitric oxide in the supernatants were increased in concentration dependent manner. The result of NO assay is consistent with those of inflammatory markers; IL-6 and IL-8 detected by PCR and ELISA. In the PCR data, IL-6 and IL-8 expressions of LPS-treated DFSCs were slightly elevated with little or no shift in the expression of TGF-β1 and TGF-β2 on conditional media. Also, protein levels of the IL-6 and IL-8 were high with LPS treatment. However, there is no change on cell viability with 100 ng/ml LPS treatment on DFSCs. During osteogenic differentiation, inflammatory cytokines, IL-6 and IL-8, were expressed with LPS treatment. LPS inhibits the extracellular calcium deposition during osteogenic differentiation of DFSCs. Also, osteocalcin expression was inhibited with LPS treatment. These findings imply that inflammation, which inevitably exists during bone healing, may be the major cause of low osteogenic differentiation. Interestingly, TGF-β1 were down-regulated and TGF-β2 were up-regulated with LPS-treated osteogenic differentiation. These higher expression of TGF-β2 on LPS-treated DFSCs reaffirmed similar trend in inflamed DFSCs.

TGF-β2 inhibitors were applied whether it could neutralize LPS-triggered inflammation which upregulate TGF-β2 on bone metabolism. Our results from alizarin red S staining and ALPase activity demonstrated that the suppression of TGF-β2 overcome the inhibited osteogenic differentiation by

LPS. With 1 μg/ml TGF-β2 inhibitors, the calcium deposits and ALP activity were increased compared to LPS-treated osteogenic differentiation. Interestingly, IL-6 and IL-8 expression triggered by LPS were suppressed by TGF-β2 inhibition. On the other hands, the osteogenic markers, Col1 and OCN, were increased with TGF-β2 inhibition. The inhibition of TGF-β2 increased the gene expression of TGF-β1. These results indicated that the inhibition of TGF-β2 suppressed the inflammatory reactions with increase of bone formation by competing with TGF-β1. These results indicated that TGF-β2 is a key factor to control both osteogenesis and inflammatory reaction.

Smad2/3 is a key regulator to demonstrate the control of both inflammation and osteogenesis. Previous researches about Smad2/3 knockout mice indicated Smad2/3 is the regulator to control the inflammation[104]. With double knockout of Smad2/3, fatal inflammation on mice were observed[105]. T cell-specific Smad signaling is essential for iTreg induction and Th suppression[50]. Previous researches demonstrated that TGF-β2 had distinct mechanism by the requirement of type III receptor, betaglycan, as co-receptor for efficient binding contrast to TGF-β1/3 by direct binding to type I and II receptors[106, 107]. Both TGF-β1/3 and TGF-β2 shared the Smad dependent signaling. In our study, Smad2/3 was phosphorylated with LPS treatment for 30 minutes on DFSCs. These proved that MSCs also were stimulated by LPS to trigger the

immune reaction. Also, the inhibition of TGF-β2 may activate Smad2/3 signaling, increasing TGF-β1 expression. The inhibition of TGF-β2 increased the gene expression of TGF-β1. Therefore, Smad2/3 activated by elevated TGF-β2 in inflammation could affect the osteogenic differentiation.

The chief raised and unresolved issue by these studies, however, is whether smad2/3 were activated by TGF-β1 or TGF-β2. While highly expressing TGF-β2 with osteogenesis on DFSCs, TGF-β1 were down-regulated. Because of relationship to TGF-β1 and osteogenesis, inhibited TGF-β1 needs to be explained on LPS-treated or Inflamed DFSCs during osteogenesis. However, this study indicated that TGF-β2 is critical point to control the bone formation on inflammation by examining the inflamed DFSCs and LPS-triggered DFSCs.

In conclusion, TGF-β2 is a key factor to understand the cause of lower levels of bone formation during inflammation. TGF-β2 can be used in both ways to explain the mechanism between bone formation and inflammation. By sharing the Smad2/3 signaling pathway, increased TGF-β2 by inflammation affects the gene expression of osteogenic related genes, osteocalcin and type I collagen, RUNX2. The results of this study suggest that the interactions of inflammation and bone formation were complexly related by TGF-β2. For future therapeutic uses of DFSCs in periodontal disease to regenerate bone

formation, the control of TGF-β2 could elicit the low levels of inflammatory reaction.

Conclusions

Inflammatory condition is considered as a crucial influencing factor on the osteogenesis. Osteogenesis of dental stem cells is suppressed by inflammatory factors/cytokines. rhBMP-2 has been used in orthopedics and dentistry at concentrations of 0.5 – 1 mg/ml. With initial burst release from high concentration of BMP-2, provoked inflammatory reactions prevent successful bone formation in surgical areas. However, there is no evidence that BMP-2

treatment causes inflammatory reactions. In this study, we found that the inflammatory environment inhibited the bone formation and the anti-inflammatory cytokine, TSG-6, secreted by mesenchymal stem cells overcome the inhibited bone formation. The level of suppression differs depending on the type of MSC, which may support expanding the use of MSCs in clinical trials, especially in bone-related diseases, by optimizing therapeutic doses of BMP-2.

Dental follicle, as a candidate source of mesenchymal stem cells, has a potential to use in the periodontal tissue regeneration. By controlling both inflammatory reaction and bone formation, the periodontal tissue can be reconstructed. With screening of inflamed dental follicle, we observed that TGF-β2 was highly increased in inflamed dental follicle, suppressing osteogenic differentiation. For the first time, this study investigated the role of TGF-β2 on inflammation and bone regenerations. By investigating the influence of human mesenchymal stem cells on inflammation, especially focusing on bone regeneration and anti-inflammatory reactions, we found the role of mesenchymal stem cells on inflammation and TGF-β2/ BMP-2 on bone formation. For future therapeutic uses of dental stem cells in periodontal disease to regenerate bone formation, the control of TGF-β2 could elicit the low levels of inflammatory reaction with secretion of TSG-6 by dental stem

cells.

References

1. Huang GT, Gronthos S, Shi S. Mesenchymal stem cells derived from dental tissues vs. those from other sources: their biology and role in regenerative medicine. J Dent Res 2009;88(9):792-806.
2. Huang RL, Yuan Y, Zou GM, et al. LPS-stimulated inflammatory environment inhibits BMP-2-induced osteoblastic differentiation through crosstalk between TLR4/MyD88/NF-kappaB and BMP/Smad signaling. Stem Cells Dev 2014;23(3):277-89.
3. Redlich K, Smolen JS. Inflammatory bone loss: pathogenesis and therapeutic intervention. Nat Rev Drug Discov 2012;11(3):234-50.
4. Stem Cells. Booklist 2007;103(22):59.
5. Gregory CA, Prockop DJ, Spees JL. Non-hematopoietic bone marrow stem cells: molecular control of expansion and differentiation. Exp Cell Res 2005;306(2):330-5.
6. Bunnell BA, Flaat M, Gagliardi C, Patel B, Ripoll C. Adipose-derived stem cells: isolation, expansion and differentiation. Methods 2008;45(2):115-20.
7. Lv C, Dai H, Sun M, et al. Mesenchymal stem cells induce epithelial mesenchymal transition in melanoma by paracrine secretion of transforming growth factor-beta. Melanoma Res 2017;27(2):74-84.
8. Mori G, Ballini A, Carbone C, et al. Osteogenic differentiation of dental follicle stem cells. Int J Med Sci 2012;9(6):480-7.
9. Acil Y, Yang F, Gulses A, et al. Isolation, characterization and investigation of differentiation potential of human periodontal ligament cells and dental follicle progenitor cells and their response to BMP-7 in vitro. Odontology 2016;104(2):123-35.
10. Shi S, Bartold PM, Miura M, et al. The efficacy of mesenchymal stem cells to regenerate and repair dental structures. Orthod Craniofac Res

2005;8(3):191-9.

11. Chang YJ, Shih DT, Tseng CP, et al. Disparate mesenchyme-lineage tendencies in mesenchymal stem cells from human bone marrow and umbilical cord blood. Stem Cells 2006;24(3):679-85.

12. Gay IC, Chen S, MacDougall M. Isolation and characterization of multipotent human periodontal ligament stem cells. Orthod Craniofac Res 2007;10(3):149-60.

13. Morsczeck CO, Drees J, Gosau M. Lipopolysaccharide from Escherichia coli but not from Porphyromonas gingivalis induce pro-inflammatory cytokines and alkaline phosphatase in dental follicle cells. Arch Oral Biol 2012;57(12):1595-601.

14. Biedermann A, Kriebel K, Kreikemeyer B, Lang H. Interactions of anaerobic bacteria with dental stem cells: an in vitro study. PLoS One 2014;9(11):e110616.

15. Liu J, Wang L, Liu W, et al. Dental follicle cells rescue the regenerative capacity of periodontal ligament stem cells in an inflammatory microenvironment. PLoS One 2014;9(9):e108752.

16. Lucaciu O, Soritau O, Gheban D, et al. Dental follicle stem cells in bone regeneration on titanium implants. BMC Biotechnol 2015;15:114.

17. Klingelhoffer C, Codrin C, Ettl T, Reichert T, Morsczeck C. miRNA-101 supports the osteogenic differentiation in human dental follicle cells. Arch Oral Biol 2016;72:47-50.

18. Seo BM, Miura M, Gronthos S, et al. Investigation of multipotent postnatal stem cells from human periodontal ligament. Lancet 2004;364(9429):149-55.

19. Vasandan AB, Shankar SR, Prasad P, et al. Functional differences in mesenchymal stromal cells from human dental pulp and periodontal ligament. J Cell Mol Med 2014;18(2):344-54.

20. Akintoye SO, Lam T, Shi S, et al. Skeletal site-specific characterization of orofacial and iliac crest human bone marrow stromal cells in same individuals. Bone 2006;38(6):758-68.

21. Morsczeck C, Gotz W, Schierholz J, et al. Isolation of precursor cells (PCs) from human dental follicle of wisdom teeth. Matrix Biol 2005;24(2):155-65.

22. Vollner F, Driemel O, Reichert T, Morsczeck C. Isolation and characterization of dental follicle precursor cells (DFPCs). J Stem Cells Regen Med 2007;2(1):130.

23. Guo L, Li J, Qiao X, et al. Comparison of odontogenic differentiation of human dental follicle cells and human dental papilla cells. PLoS One 2013;8(4):e62332.

24. Chen D, Zhao M, Mundy GR. Bone morphogenetic proteins. Growth Factors 2004;22(4):233-41.

25. Tumialan LM, Pan J, Rodts GE, Mummaneni PV. The safety and efficacy of anterior cervical discectomy and fusion with polyetheretherketone spacer and recombinant human bone morphogenetic protein-2: a review of 200 patients. J Neurosurg Spine 2008;8(6):529-35.

26. Wei S, Cai X, Huang J, et al. Recombinant human BMP-2 for the treatment of open tibial fractures. Orthopedics 2012;35(6):e847-54.

27. Boyne PJ, Lilly LC, Marx RE, et al. De novo bone induction by recombinant human bone morphogenetic protein-2 (rhBMP-2) in maxillary sinus floor augmentation. J Oral Maxillofac Surg 2005;63(12):1693-707.

28. Swiontkowski MF, Aro HT, Donell S, et al. Recombinant human bone morphogenetic protein-2 in open tibial fractures. A subgroup analysis of data combined from two prospective randomized studies. J Bone Joint Surg Am 2006;88(6):1258-65.

29. Fiorellini JP, Howell TH, Cochran D, et al. Randomized study evaluating recombinant human bone morphogenetic protein-2 for extraction socket augmentation. J Periodontol 2005;76(4):605-13.
30. Agrawal V, Sinha M. A review on carrier systems for bone morphogenetic protein-2. J Biomed Mater Res B Appl Biomater 2017;105(4):904-25.
31. Guan J, Zhang J, Zhu Z, et al. Bone morphogenetic protein 2 gene transduction enhances the osteogenic potential of human urine-derived stem cells. Stem Cell Res Ther 2015;6:5.
32. Zara JN, Siu RK, Zhang X, et al. High doses of bone morphogenetic protein 2 induce structurally abnormal bone and inflammation in vivo. Tissue Eng Part A 2011;17(9-10):1389-99.
33. Perri B, Cooper M, Lauryssen C, Anand N. Adverse swelling associated with use of rh-BMP-2 in anterior cervical discectomy and fusion: a case study. Spine J 2007;7(2):235-9.
34. Shields LB, Raque GH, Glassman SD, et al. Adverse effects associated with high-dose recombinant human bone morphogenetic protein-2 use in anterior cervical spine fusion. Spine (Phila Pa 1976) 2006;31(5):542-7.
35. Lee KB, Murray SS, Taghavi CE, et al. Bone morphogenetic protein-binding peptide reduces the inflammatory response to recombinant human bone morphogenetic protein-2 and recombinant human bone morphogenetic protein-7 in a rodent model of soft-tissue inflammation. Spine J 2011;11(6):568-76.
36. Smucker JD, Rhee JM, Singh K, Yoon ST, Heller JG. Increased swelling complications associated with off-label usage of rhBMP-2 in the anterior cervical spine. Spine (Phila Pa 1976) 2006;31(24):2813-9.
37. Toth JM, Boden SD, Burkus JK, et al. Short-term osteoclastic activity induced by locally high concentrations of recombinant human bone

morphogenetic protein-2 in a cancellous bone environment. Spine (Phila Pa 1976) 2009;34(6):539-50.

38. Vaidya R, Carp J, Sethi A, et al. Complications of anterior cervical discectomy and fusion using recombinant human bone morphogenetic protein-2. Eur Spine J 2007;16(8):1257-65.

39. Carragee EJ, Hurwitz EL, Weiner BK. A critical review of recombinant human bone morphogenetic protein-2 trials in spinal surgery: emerging safety concerns and lessons learned. Spine J 2011;11(6):471-91.

40. Talati M, West J, Zaynagetdinov R, et al. BMP pathway regulation of and by macrophages. PLoS One 2014;9(4):e94119.

41. Simoes Sato AY, Bub GL, Campos AH. BMP-2 and -4 produced by vascular smooth muscle cells from atherosclerotic lesions induce monocyte chemotaxis through direct BMPRII activation. Atherosclerosis 2014;235(1):45-55.

42. Lee GT, Kwon SJ, Lee JH, et al. Induction of interleukin-6 expression by bone morphogenetic protein-6 in macrophages requires both SMAD and p38 signaling pathways. J Biol Chem 2010;285(50):39401-8.

43. Mundy GR. Osteoporosis and inflammation. Nutr Rev 2007;65(12 Pt 2):S147-51.

44. Shen J, James AW, Zara JN, et al. BMP2-induced inflammation can be suppressed by the osteoinductive growth factor NELL-1. Tissue Eng Part A 2013;19(21-22):2390-401.

45. Massague J. TGFbeta signalling in context. Nat Rev Mol Cell Biol 2012;13(10):616-30.

46. Krzemien S, Knapczyk P. [Current review on the role of transforming growth factor beta (TGF-beta) in some pathological disorders]. Wiad Lek 2005;58(9-10):536-9.

47. Zhen G, Wen C, Jia X, et al. Inhibition of TGF-beta signaling in mesenchymal stem cells of subchondral bone attenuates osteoarthritis. Nat Med 2013;19(6):704-12.

48. Li MO, Flavell RA. Contextual regulation of inflammation: a duet by transforming growth factor-beta and interleukin-10. Immunity 2008;28(4):468-76.

49. Grafe I, Yang T, Alexander S, et al. Excessive transforming growth factor-beta signaling is a common mechanism in osteogenesis imperfecta. Nat Med 2014;20(6):670-5.

50. Yoshimura A, Wakabayashi Y, Mori T. Cellular and molecular basis for the regulation of inflammation by TGF-beta. J Biochem 2010;147(6):781-92.

51. Ma S, Xie N, Li W, et al. Immunobiology of mesenchymal stem cells. Cell Death Differ 2014;21(2):216-25.

52. Alliston T, Choy L, Ducy P, Karsenty G, Derynck R. TGF-beta-induced repression of CBFA1 by Smad3 decreases cbfa1 and osteocalcin expression and inhibits osteoblast differentiation. EMBO J 2001;20(9):2254-72.

53. Kang JS, Alliston T, Delston R, Derynck R. Repression of Runx2 function by TGF-beta through recruitment of class II histone deacetylases by Smad3. EMBO J 2005;24(14):2543-55.

54. Moioli EK, Hong L, Mao JJ. Inhibition of osteogenic differentiation of human mesenchymal stem cells. Wound Repair Regen 2007;15(3):413-21.

55. Critchlow MA, Bland YS, Ashhurst DE. The effect of exogenous transforming growth factor-beta 2 on healing fractures in the rabbit. Bone 1995;16(5):521-7.

56. Hering S, Isken E, Knabbe C, et al. TGFbeta1 and TGFbeta2 mRNA and protein expression in human bone samples. Exp Clin Endocrinol

Diabetes 2001;109(4):217-26.

57. Seo T, Cha S, Kim TI, Lee JS, Woo KM. Porphyromonas gingivalis-derived lipopolysaccharide-mediated activation of MAPK signaling regulates inflammatory response and differentiation in human periodontal ligament fibroblasts. J Microbiol 2012;50(2):311-9.

58. Kato H, Taguchi Y, Tominaga K, Umeda M, Tanaka A. Porphyromonas gingivalis LPS inhibits osteoblastic differentiation and promotes pro-inflammatory cytokine production in human periodontal ligament stem cells. Arch Oral Biol 2014;59(2):167-75.

59. Kim DS, Shin MR, Kim YS, et al. Anti-inflammatory effects of glutamine on LPS-stimulated human dental pulp cells correlate with activation of MKP-1 and attenuation of the MAPK and NF-kappaB pathways. Int Endod J 2015;48(3):220-8.

60. Li C, Li B, Dong Z, et al. Lipopolysaccharide differentially affects the osteogenic differentiation of periodontal ligament stem cells and bone marrow mesenchymal stem cells through Toll-like receptor 4 mediated nuclear factor kappaB pathway. Stem Cell Res Ther 2014;5(3):67.

61. Nemeth K, Leelahavanichkul A, Yuen PS, et al. Bone marrow stromal cells attenuate sepsis via prostaglandin E(2)-dependent reprogramming of host macrophages to increase their interleukin-10 production. Nat Med 2009;15(1):42-9.

62. Castro-Manrreza ME, Mayani H, Monroy-Garcia A, et al. Human mesenchymal stromal cells from adult and neonatal sources: a comparative in vitro analysis of their immunosuppressive properties against T cells. Stem Cells Dev 2014;23(11):1217-32.

63. Kim J, Hematti P. Mesenchymal stem cell-educated macrophages: a novel type of alternatively activated macrophages. Exp Hematol 2009;37(12):1445-53.

64. Liu M, Zeng X, Wang J, et al. Immunomodulation by mesenchymal stem cells in treating human autoimmune disease-associated lung fibrosis. Stem Cell Res Ther 2016;7(1):63.

65. Nazarov C, Lo Surdo J, Bauer SR, Wei CH. Assessment of immunosuppressive activity of human mesenchymal stem cells using murine antigen specific CD4 and CD8 T cells in vitro. Stem Cell Res Ther 2013;4(5):128.

66. Kim BC, Bae H, Kwon IK, et al. Osteoblastic/cementoblastic and neural differentiation of dental stem cells and their applications to tissue engineering and regenerative medicine. Tissue Eng Part B Rev 2012;18(3):235-44.

67. Luz-Crawford P, Noel D, Fernandez X, et al. Mesenchymal stem cells repress Th17 molecular program through the PD-1 pathway. PLoS One 2012;7(9):e45272.

68. Gerdoni E, Gallo B, Casazza S, et al. Mesenchymal stem cells effectively modulate pathogenic immune response in experimental autoimmune encephalomyelitis. Ann Neurol 2007;61(3):219-27.

69. Kang HS, Habib M, Chan J, et al. A paradoxical role for IFN-gamma in the immune properties of mesenchymal stem cells during viral challenge. Exp Hematol 2005;33(7):796-803.

70. Djouad F, Fritz V, Apparailly F, et al. Reversal of the immunosuppressive properties of mesenchymal stem cells by tumor necrosis factor alpha in collagen-induced arthritis. Arthritis Rheum 2005;52(5):1595-603.

71. Aggarwal S, Pittenger MF. Human mesenchymal stem cells modulate allogeneic immune cell responses. Blood 2005;105(4):1815-22.

72. Krampera M, Cosmi L, Angeli R, et al. Role for interferon-gamma in the immunomodulatory activity of human bone marrow mesenchymal stem cells. Stem Cells 2006;24(2):386-98.

73. Lee RH, Pulin AA, Seo MJ, et al. Intravenous hMSCs improve myocardial infarction in mice because cells embolized in lung are activated to secrete the anti-inflammatory protein TSG-6. Cell Stem Cell 2009;5(1):54-63.

74. Lee RH, Yu JM, Foskett AM, et al. TSG-6 as a biomarker to predict efficacy of human mesenchymal stem/progenitor cells (hMSCs) in modulating sterile inflammation in vivo. Proc Natl Acad Sci U S A 2014;111(47):16766-71.

75. Tang Y, Wu X, Lei W, et al. TGF-beta1-induced migration of bone mesenchymal stem cells couples bone resorption with formation. Nat Med 2009;15(7):757-65.

76. Tang SY, Alliston T. Regulation of postnatal bone homeostasis by TGFbeta. Bonekey Rep 2013;2:255.

77. Thesleff I, Sharpe P. Signalling networks regulating dental development. Mechanisms of Development 1997;67(2):111-23.

78. Hong JH, Lee GT, Lee JH, et al. Effect of bone morphogenetic protein-6 on macrophages. Immunology 2009;128(1 Suppl):e442-50.

79. Manolagas SC, Jilka RL. Bone marrow, cytokines, and bone remodeling. Emerging insights into the pathophysiology of osteoporosis. N Engl J Med 1995;332(5):305-11.

80. Teitelbaum SL. Bone resorption by osteoclasts. Science 2000;289(5484):1504-8.

81. Hume DA, Ross IL, Himes SR, et al. The mononuclear phagocyte system revisited. J Leukoc Biol 2002;72(4):621-7.

82. Haynes DR, Crotti TN, Loric M, et al. Osteoprotegerin and receptor activator of nuclear factor kappaB ligand (RANKL) regulate osteoclast formation by cells in the human rheumatoid arthritic joint. Rheumatology (Oxford) 2001;40(6):623-30.

83. Yu B, Sondag GR, Malcuit C, Kim MH, Safadi FF. Macrophage-

Associated Osteoactivin/GPNMB Mediates Mesenchymal Stem Cell Survival, Proliferation, and Migration Via a CD44-Dependent Mechanism. J Cell Biochem 2016;117(7):1511-21.

84. Pirraco RP, Reis RL, Marques AP. Effect of monocytes/macrophages on the early osteogenic differentiation of hBMSCs. J Tissue Eng Regen Med 2013;7(5):392-400.

85. Takabayashi H, Shinohara M, Mao M, et al. Anti-inflammatory activity of bone morphogenetic protein signaling pathways in stomachs of mice. Gastroenterology 2014;147(2):396-406 e7.

86. Krötzsch E, Salgado, R.M., Caba, D.,Lichtinger, A., Padilla, L., Di Silvio, M. . Alkaline phosphatase activity is related to acute inflammation and collagen turnover during acute and chronic wound healing. Wound Repair and Regeneration 2005;13(2):A44-A44.

87. Shead EF, Haworth CS, Barker H, Bilton D, Compston JE. Osteoclast function, bone turnover and inflammatory cytokines during infective exacerbations of cystic fibrosis. J Cyst Fibros 2010;9(2):93-8.

88. Lee KB, Taghavi CE, Song KJ, et al. Inflammatory characteristics of rhBMP-2 in vitro and in an in vivo rodent model. Spine (Phila Pa 1976) 2011;36(3):E149-54.

89. Lee KB, Taghavi CE, Murray SS, et al. BMP induced inflammation: a comparison of rhBMP-7 and rhBMP-2. J Orthop Res 2012;30(12):1985-94.

90. Huang RL, Yuan Y, Tu J, Zou GM, Li Q. Opposing TNF-alpha/IL-1beta- and BMP-2-activated MAPK signaling pathways converge on Runx2 to regulate BMP-2-induced osteoblastic differentiation. Cell Death Dis 2014;5:e1187.

91. Hegyi B, Kornyei Z, Ferenczi S, et al. Regulation of mouse microglia activation and effector functions by bone marrow-derived mesenchymal stem cells. Stem Cells Dev 2014;23(21):2600-12.

92. Choi H, Lee RH, Bazhanov N, Oh JY, Prockop DJ. Anti-inflammatory protein TSG-6 secreted by activated MSCs attenuates zymosan-induced mouse peritonitis by decreasing TLR2/NF-kappaB signaling in resident macrophages. Blood 2011;118(2):330-8.

93. Prockop DJ, Oh JY. Medical therapies with adult stem/progenitor cells (MSCs): a backward journey from dramatic results in vivo to the cellular and molecular explanations. J Cell Biochem 2012;113(5):1460-9.

94. Gibon E, Lu L, Goodman SB. Aging, inflammation, stem cells, and bone healing. Stem Cell Res Ther 2016;7(1):44.

95. Wang N, Shao Y, Mei Y, et al. Novel mechanism for mesenchymal stem cells in attenuating peritoneal adhesion: accumulating in the lung and secreting tumor necrosis factor alpha-stimulating gene-6. Stem Cell Res Ther 2012;3(6):51.

96. Lee RH, Seo MJ, Pulin AA, et al. The CD34-like protein PODXL and alpha6-integrin (CD49f) identify early progenitor MSCs with increased clonogenicity and migration to infarcted heart in mice. Blood 2009;113(4):816-26.

97. Manning CN, Martel C, Sakiyama-Elbert SE, et al. Adipose-derived mesenchymal stromal cells modulate tendon fibroblast responses to macrophage-induced inflammation in vitro. Stem Cell Res Ther 2015;6:74.

98. Lee DE, Ayoub N, Agrawal DK. Mesenchymal stem cells and cutaneous wound healing: novel methods to increase cell delivery and therapeutic efficacy. Stem Cell Res Ther 2016;7(1):37.

99. Sullivan CB, Porter RM, Evans CH, et al. TNFalpha and IL-1beta influence the differentiation and migration of murine MSCs independently of the NF-kappaB pathway. Stem Cell Res Ther 2014;5(4):104.

100. Mahoney DJ, Mikecz K, Ali T, et al. TSG-6 regulates bone remodeling through inhibition of osteoblastogenesis and osteoclast activation. J Biol Chem 2008;283(38):25952-62.

101. Lee JH, Lin JD, Fong JI, Ryder MI, Ho SP. The adaptive nature of the bone-periodontal ligament-cementum complex in a ligature-induced periodontitis rat model. Biomed Res Int 2013;2013:876316.

102. Zhang Q, Chen B, Yan F, et al. Interleukin-10 inhibits bone resorption: a potential therapeutic strategy in periodontitis and other bone loss diseases. Biomed Res Int 2014;2014:284836.

103. Xu C, Yu P, Han X, et al. TGF-beta promotes immune responses in the presence of mesenchymal stem cells. J Immunol 2014;192(1):103-9.

104. Sugiyama Y, Kakoi K, Kimura A, et al. Smad2 and Smad3 are redundantly essential for the suppression of iNOS synthesis in macrophages by regulating IRF3 and STAT1 pathways. Int Immunol 2012;24(4):253-65.

105. Takimoto T, Wakabayashi Y, Sekiya T, et al. Smad2 and Smad3 are redundantly essential for the TGF-beta-mediated regulation of regulatory T plasticity and Th1 development. J Immunol 2010;185(2):842-55.

106. Zuniga JE, Groppe JC, Cui Y, et al. Assembly of TbetaRI:TbetaRII:TGFbeta ternary complex in vitro with receptor extracellular domains is cooperative and isoform-dependent. J Mol Biol 2005;354(5):1052-68.

107. Jaschinski F, Rothhammer T, Jachimczak P, et al. The antisense oligonucleotide trabedersen (AP 12009) for the targeted inhibition of TGF-beta2. Curr Pharm Biotechnol 2011;12(12):2203-13.

Table and Figures

Table 1. Reverse transcription-polymerase chain reaction (RT-PCR) primer sequences

Gene	Primer Sequence
ALK2 forward	5′-GCA TTC CCA GAG CAC CAA TC -3′
ALK2 reverse	5′-CTG TGA GTC TTG CGG ATG GA -3′
ALK3 forward	5′-GCA TAA CTA ATG GAC ATT GCT -3′
ALK3 reverse	5′-TAG AGT TTC TCC TCC GAT GG -3′
ALK6 forward	5′-GCA GCA CAG ACG GAT ATT GT -3′
ALK6 reverse	5′-TTT CAT GCC TCA TCA ACA CT -3′
Act-RIIA forward	5′-ATG GCT AGA GGA TTG GCA TAT T -3′
Act-RIIA reverse	5′-TCT TCA ATG GTT TCA CAG AGC A -3′
Act-RIIB forward	5′-ACA GGT AGG CAC GAG ACG GT -3′
Act-RIIB reverse	5′-GTA GTG CCG TTG ACC GAC CT -3′
BMP-RII forward	5′-ACG GGA GAG AAG ACG AGC CT -3′
BMP-RII reverse	5′-CTA GAT CAA GAG AGG GTT CG -3′
CD14 forward	5’-TCT CTG TCC CCA CAA GTT CC-3’
CD14 reverse	5’-CCC GTC CAG TGT CAG GTT ATC-3’
CD68 forward	5’-GAA CCC CAA CAA AAC CAA G-3’
CD68 reverse	5’-GAT GAG AGG CAG CAA GAT G-3’
TNF-a forward	5’-AGC CCA TGT TGT AGC AAA CC-3
TNF-a reverse	5’-TGA GGT ACA GGC CCT CTG AT-3
IL-8 forward	5’-ACT GAG AGT GAT TGA GAG TGG AC-3’
IL-8 reverse	5’-AAC CCT CTG CAC CCA GTT TTC-3’
IL-1β forward	5’-TCA TTG CTC AAG TGT CTG AAG C-3’

IL-1β reverse	5’-TGG TCG GAG ATT CGT AGC-3’
GAPDH forward	5’-AGCCGCATCTTCTTTTGCGTC-3’
GAPDH reverse	5’-TCATATTTGGCAGGTTTTTCT-3’

Abbreviations: ALK, activin receptor-like kinase; Act, activin; BMP, bone morphogenetic protein; TNF, tumor necrosis factor; IL, interleukin; R, receptor.

Table 2. Mass Spectrometry Analysis by comparison of normal and inflamed dental follicle in different bands of 1D-SDS-PAGE gel. Proteins identified by LC-MS/MS (liquid chromatography-coupled electrospray ionization MS/MS) were searched against the NCBI database using the MASCOT search software. The list includes all significant hits.

Sample	Number	NCBI BLAST	Protein name	MASCOT Score	Mass (Da)
Normal	1	GI:5821385	MTH1a (p26) [Homo sapiens]	95	22537
DF	2	GI:82571735	PPIF protein [Homo sapiens]	71	16530
	3	GI:284164	arginine-rich protein - human	63	26889
	4	GI:5031851	stathmin isoform a [Homo sapiens]	59	17292
	5	GI:223480	dismutase, Cu/Zn superoxide	53	15792
	6	GI:18490199	TWF1 protein [Homo sapiens]	50	28805
	7	GI:385719190	layilin isoform 3 [Homo sapiens]	38	25555
	8	GI:5453678	epididymal secretory protein E1 precursor [Homo sapiens]	38	16559
	9	GI:30506	desmoglein type 1 [Homo sapiens]	32	113644
	10	GI:9502027	nucleotide binding protein [Homo sapiens]	27	30204
	11	GI:57997547	hypothetical protein [Homo sapiens]	37	13865
	12	GI:3318841	Chain A, Horf6 A Novel Human Peroxidase Enzyme	34	25011
	13	GI:4503987	gamma-glutamyl hydrolase precursor [Homo sapiens]	77	35941
	14	GI:31291	unnamed protein product [Homo sapiens]	70	38589
	15	GI:34234	laminin-binding protein [Homo sapiens]	55	31774
	16	GI:16549132	unnamed protein product [Homo sapiens]	54	60904
	17	GI:6912682	spondin-2 precursor [Homo sapiens]	40	35750
	18	GI:49256867	RAD50 protein, partial [Homo sapiens]	29	84003
	19	GI:18376667	hSSH-2A [Homo sapiens]	27	21650

Inflamed DF	1	GI:36038	rho GDP dissociation inhibitor (GDI) [Homo sapiens]	54	23179
	2	GI:4808278	lanosterol synthase [Homo sapiens]	33	83225
	3	GI:4506193	proteasome subunit beta type-1 [Homo sapiens]	137	26472
	4	GI:4506181	proteasome subunit alpha type-2 [Homo sapiens]	89	25882
	5	GI:21465651	Chain J, Crystal Structure Of The Mammalian 20s Proteasome At 2.75 A Resolution	84	22915
	6	GI:31543380	protein DJ-1 [Homo sapiens]	81	19878
	7	GI:4506243	polypyrimidine tract-binding protein 1 isoform a [Homo sapiens]	79	59596
	8	GI:4504447	heterogeneous nuclear ribonucleoproteins A2/B1 isoform A2 [Homo sapiens]	69	35984
	9	GI:348239	unnamed protein product [Homo sapiens]	50	54233
	10	GI:178775	proapolipoprotein, partial [Homo sapiens]	44	28944
	11	GI:179462	N-acetyl-beta-glucosaminidase prepro-polypeptide, partial [Homo sapiens]	44	64321
	12	GI:31189	unnamed protein product [Homo sapiens]	36	23182
	13	GI:182399	farnesyl pyrophosphate synthetase (EC 2.5.1.1) [Homo sapiens]	64	40495
	14	GI:557563	transforming growth factor beta 2 [Homo sapiens]	41	47603
	15	GI:3294548	cathepsin Z precursor [Homo sapiens]	40	33860
	16	GI:33431109	transforming growth factor beta 1 [Homo sapiens]	39	12908
	17	GI:10798804	sperm antigen [Homo sapiens]	29	84869

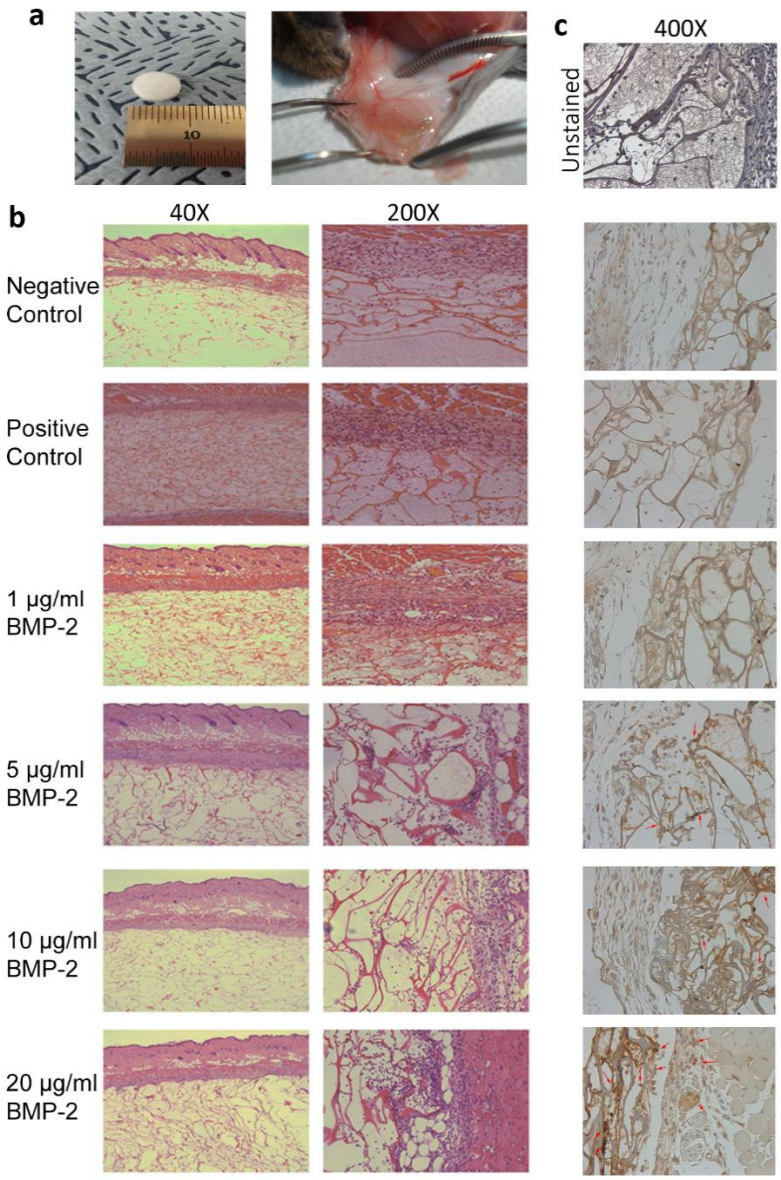
a
10
c
400X
Unstained
b
40X
200X
Negative Control
Positive Control
1 μg/ml BMP-2
5 μg/ml BMP-2
10 μg/ml BMP-2
20 μg/ml BMP-2

Figure 1. High concentrations of BMP-2 triggered the infiltration of immune cells from blood vessels. (a) Collagen sponges (8 mm in diameter, 1 mm in thickness) as carriers were transplanted with 1, 5, 10, and 20 μg/ml BMP-2 on the dorsum of mouse. (b) After 24 hours, inflammatory cells were identified on the swollen soft tissue near the implanted collagen sponge with BMP-2 in H & E staining. (c) To detect infiltrated activated macrophages, immunohistochemistry was performed via staining with F4/80 antibody (Abcam 100790, 1:100). The red arrow indicated activated macrophages (400x).

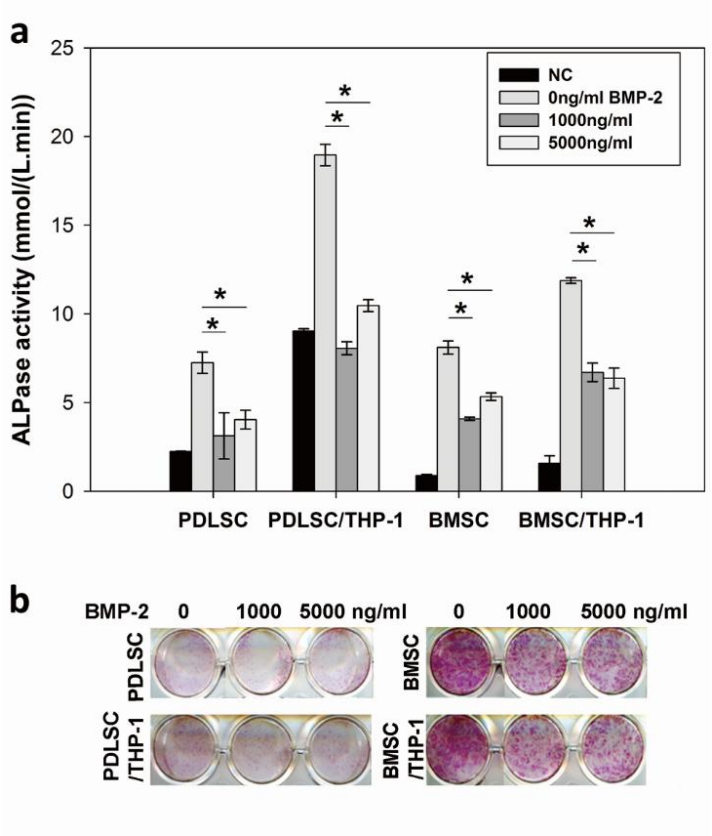

Figure 2. Osteoblastic differentiation of MSCs is inhibited by a high BMP-2 concentration. (a**)** ALPase activity from dental MSCs cultured alone or with THP-1 cells. THP-1 cells co-cultured with BMSCs/PDLSCs or monocultured THP-1 cells were incubated in osteogenic medium with 1,000 ng/ml or 5,000 ng/ml of BMP-2 for 5 days. **(b)** ALPase protein was detected by staining on day 5 using ALPase staining. Abbreviations: NC, negative control with no osteogenic differentiation. Each bar represents the mean ± S.E. of three independent experiment. *P<0.05 compared with the control group, n=3.

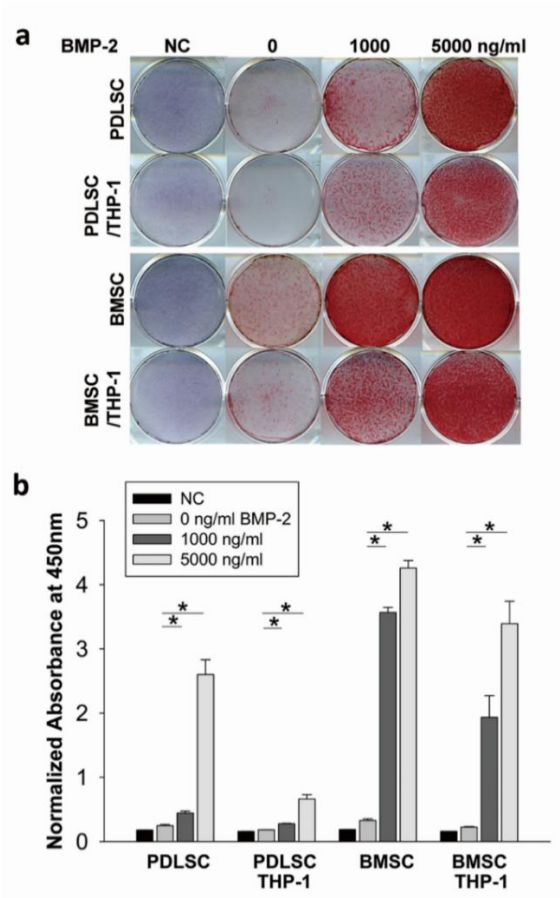

Figure 3. Co-culturing THP-1 cells inhibits late osteogenic differentiation of dental mesenchymal stem cells. (a) Calcium deposits from osteogenic differentiation of both BMSCs and PDLSCs with or without THP-1 cells were stained with alizarin red S solution at day 10. (b) Stained calcium deposits were destained and quantified with 20% methanol and 10% acetic acid. Abbreviations: NC, negative control with no osteogenic differentiation. Each bar represents the mean ± S.E. of three independent experiment. *P<0.05 compared with the control group, n=3.

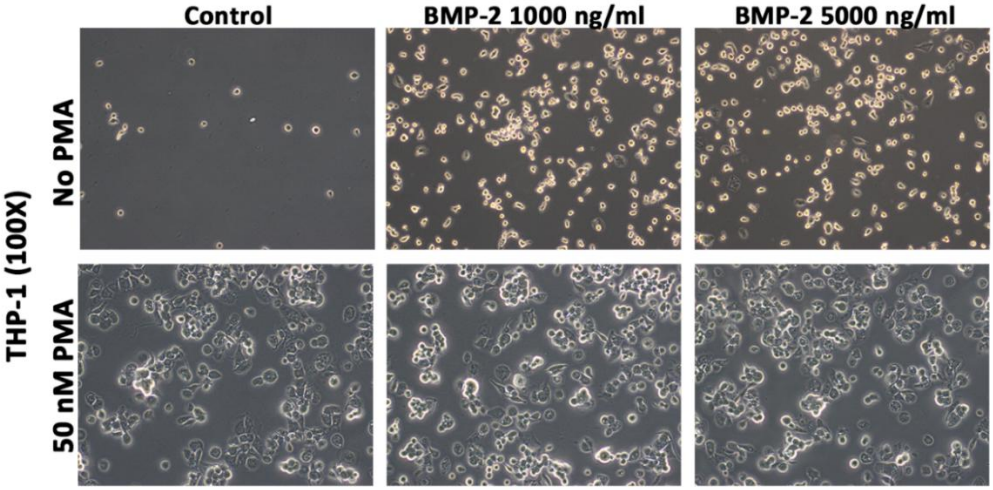

Figure 4. Morphology of THP-1 cells. Without PMA stimulation, THP-1 cells alone cannot be stimulated with BMP-2 treatment.

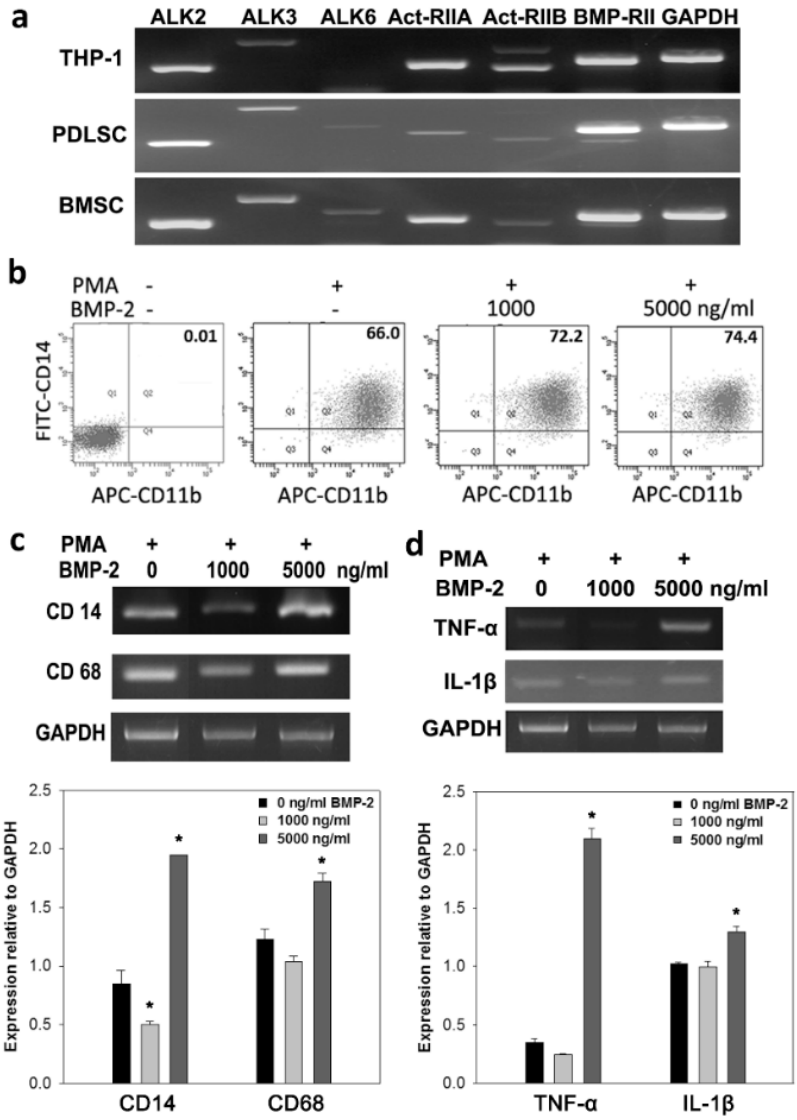
a
ALK2
ALK3
ALK6
Act-RIIA
Act-RIIB
BMP-RII
GAPDH
THP-1
PDLSC
BMSC
b
PMA - + + +
BMP-2 - - 1000 5000 ng/ml
0.01
66.0
72.2
74.4
FITC-CD14
APC-CD11b
c
PMA + + +
BMP-2 0 1000 5000 ng/ml
CD 14
CD 68
GAPDH
d
PMA + + +
BMP-2 0 1000 5000 ng/ml
TNF-α
IL-1β
GAPDH
0 ng/ml BMP-2
1000 ng/ml
5000 ng/ml
Expression relative to GAPDH
CD14
CD68
TNF-α
IL-1β

Figure 5. Characteristics of THP-1 cells in BMP-2-induced inflammation. (a) RT-PCR showed that MSCs and PMA-stimulated THP-1 cells had different levels of BMP receptors, although there were some similarities. (b) Flow cytometric analysis of CD14 and CD11b expression in THP-1 cells. Results for THP-1 activated with 50 nM PMA for 3 days followed by BMP-2 for 1 day were obtained using fluorescein isothiocyanate (FITC)-conjugated anti-human CD14, and allophycocyanin (APC)-conjugated anti-human CD11b, surface markers of mature macrophages. The number of CD14 and CD11b double-positive cells was increased by BMP-2 treatment, regardless of dose. (c) RT-PCR for macrophage markers (CD14 and CD68) on THP-1 cells after treatment with various BMP-2 concentrations. Gene expression was normalized with GAPDH per sample. (d) Gene expression determined by RT-PCR. IL-1β and TNF-α gene expression relative to GAPDH were measured after culture with various BMP-2 concentrations for 24 hours. (n=3). Each bar represents the mean ± S.E. *$P<0.05$ compared with the control group.

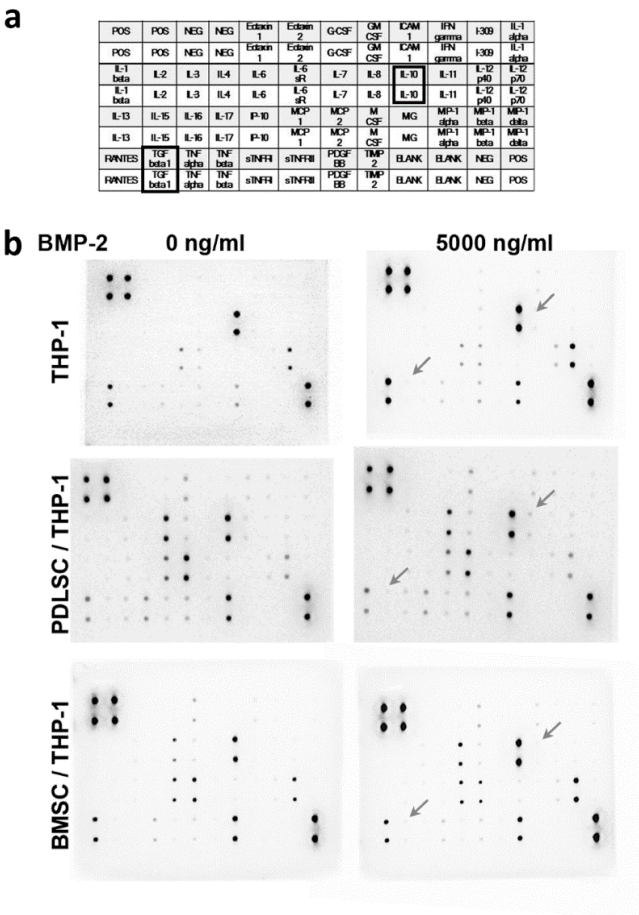

Figure 6. Antibody array of THP-1 cells with or without PDLSC/BMSCs. (A) Array map. POS (positive control spot), NEG (negative control spot), BLANK (blank spot) (B) THP-1 cells were activated with 50 nM PMA for 3 days and triggered with 5,000 ng/ml BMP-2 for 24 hours. Inflammatory cytokine expression was enhanced upon BMP-2 induction. Co-culturing MSCs and THP-1 cells resulted in lower levels of inflammatory cytokines than in THP-1 cells alone. Arrows indicate anti-inflammatory cytokines, such as IL-10 and TGF-β1.

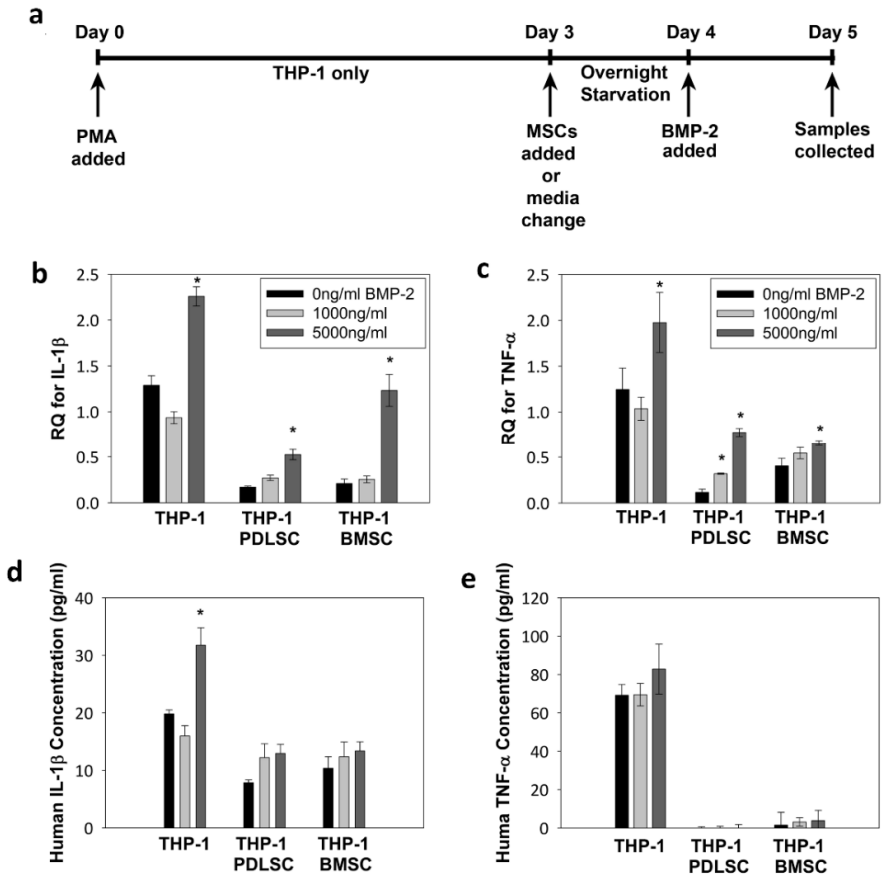

Figure 7. MSCs suppress the expression of inflammatory cytokines in the presence of various BMP-2 concentrations. (a) Experimental scheme. Samples were collected for ELISA and real-time PCR. (b, c) Real-time RT-PCR (n=3) normalized to GAPDH expression showed that the expression of IL-1β and TNF-α was blocked by 24-hour co-culture of MSCs with PMA-stimulated THP-1 cells. (d, e) ELISA assay (n=4) for IL-1β and TNF-α in supernatants following BMP-2 treatment for 24 hours. Each bar represents the mean ± S.E. *P<0.05 compared with the control group.

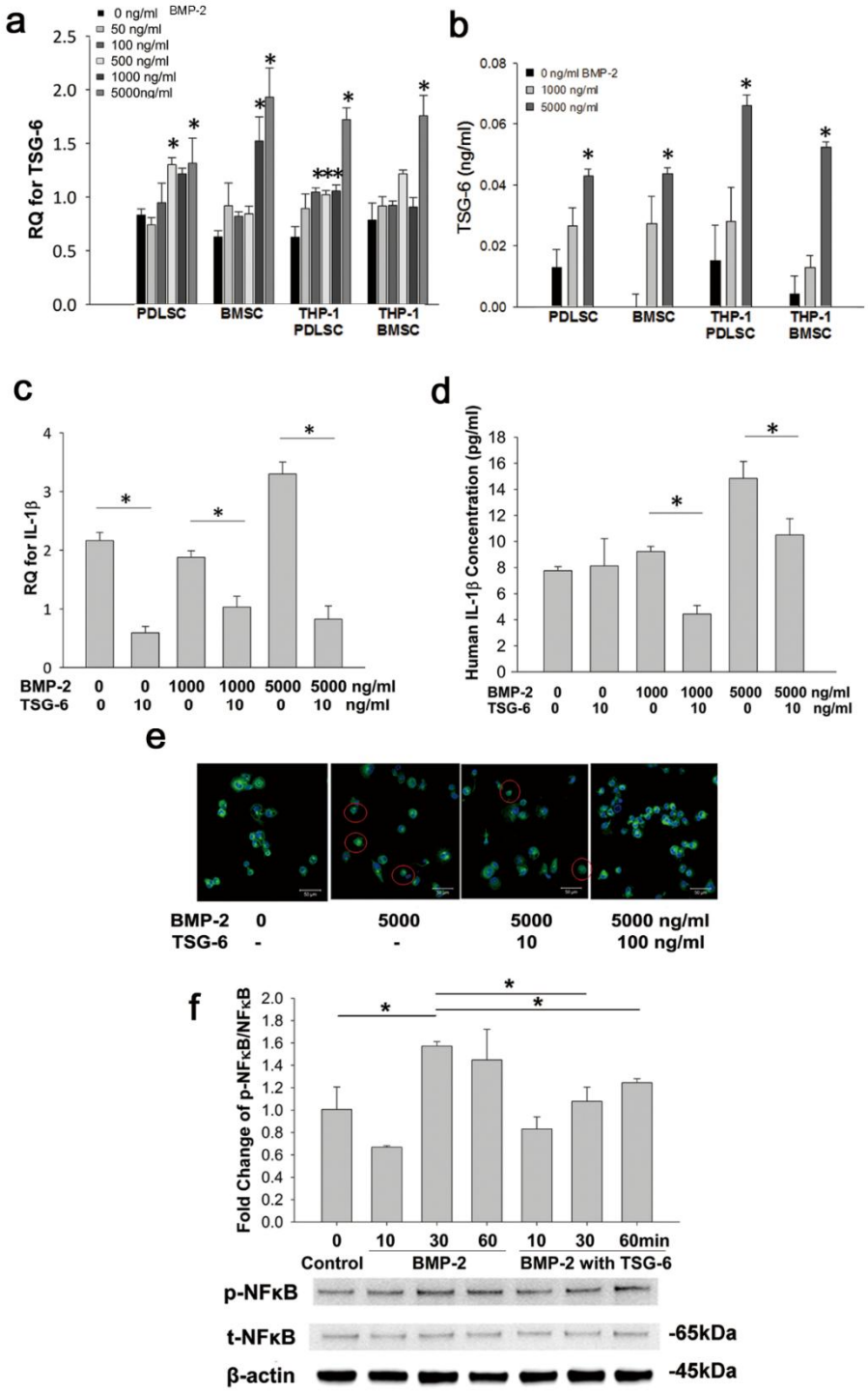
a
0 ng/ml BMP-2
50 ng/ml
100 ng/ml
500 ng/ml
1000 ng/ml
5000ng/ml
RQ for TSG-6
PDLSC
BMSC
THP-1 PDLSC
THP-1 BMSC
b
0 ng/ml BMP-2
1000 ng/ml
5000 ng/ml
TSG-6 (ng/ml)
c
RQ for IL-1β
BMP-2 0 0 1000 1000 5000 5000 ng/ml
TSG-6 0 10 0 10 0 10 ng/ml
d
Human IL-1β Concentration (pg/ml)
e
BMP-2 0 5000 5000 5000 ng/ml
TSG-6 - - 10 100 ng/ml
f
Fold Change of p-NFκB/NFκB
0 10 30 60 10 30 60min
Control BMP-2 BMP-2 with TSG-6
p-NFκB
t-NFκB
β-actin
-65kDa
-45kDa

Figure 8. TSG-6 secreted by MSCs in response to BMP-2 induction interferes with the inflammatory reactions of THP-1 cells through NF-κB signaling. (a) Real-time RT-PCR revealed that PDLSCs and BMSCs in the presence or absence of THP-1 cells secreted TSG-6 in response to BMP-2 treatment for 24 hours, as normalized to GAPDH. (b) The quantitative measurement of human TSG-6 was performed with an ELISA kit. Levels of TSG-6 were measured upon BMP-2 treatment for 24 hours. (c, d) Real-time analysis and ELISA showed that TSG-6 inhibited IL-1β expression in THP-1 cells. THP-1 cells were exposed to 50 nM PMA for 3 days and with 1,000 ng/ml or 5,000 ng/ml BMP-2 and 10 ng/ml TSG-6 for 24 hours. (e) Immunofluorescence analysis of NF-κB. THP-1 cells were pre-stimulated with 50 nM PMA and then exposed to BMP-2 for 3 hours in the presence of 10 or 100 ng/ml TSG-6. NF-κB translocation into the nucleus (RED circle) was decreased by TSG-6 treatment. Magnification 200X. Scale bar is 50 μm. (f) Western blots were performed to measure NF-kB phosphorylation. THP-1 cells were stimulated with 50 nM PMA and treated with 5,000 ng/ml BMP-2 or 10 ng/ml TSG-6 for 10, 30, or 60 minutes. Proteins were collected and the ratio of phospho-NF-kB to total NF-kB was determined by immunoblotting. The immunoblot data were normalized to β-actin. Each bar represents the mean ± S.E. *$P<0.05$ compared with the control group, n=3.

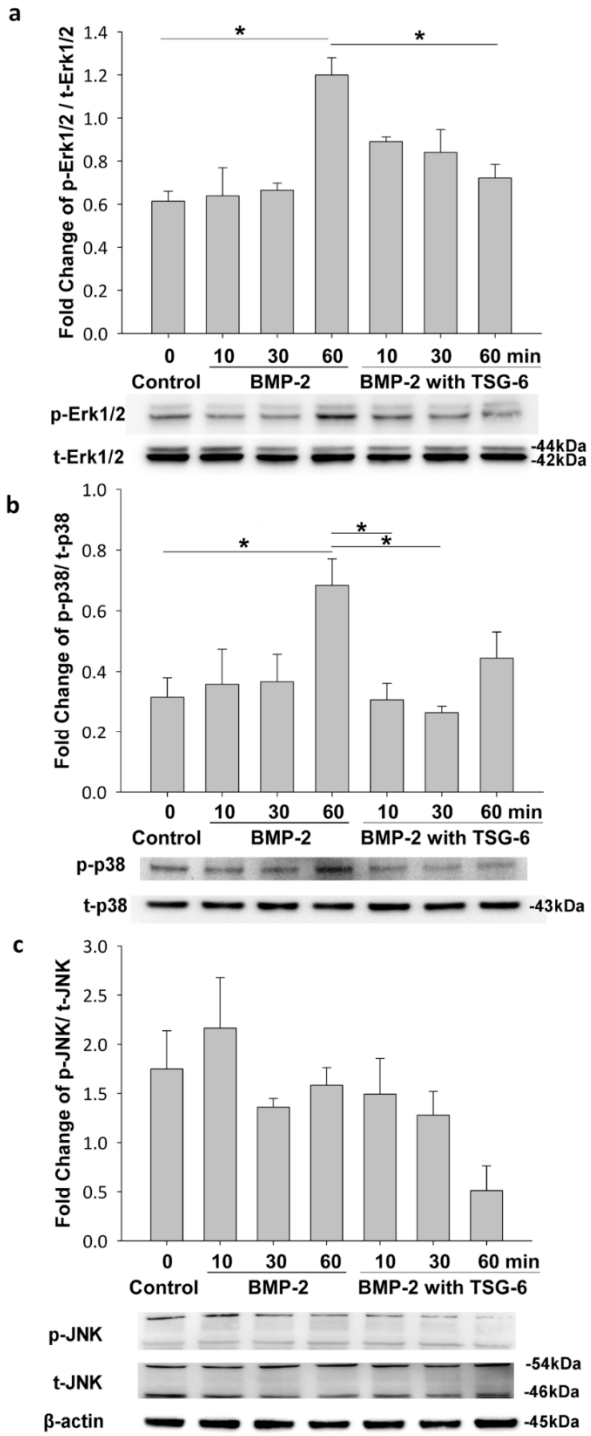
a
Fold Change of p-Erk1/2 / t-Erk1/2
1.4
1.2
1.0
0.8
0.6
0.4
0.2
0.0
*
*
0
10
30
60
10
30
60 min
Control
BMP-2
BMP-2 with TSG-6
p-Erk1/2
t-Erk1/2
-44kDa
-42kDa
b
Fold Change of p-p38/ t-p38
1.0
0.8
0.6
0.4
0.2
0.0
*
*
*
0
10
30
60
10
30
60 min
Control
BMP-2
BMP-2 with TSG-6
p-p38
t-p38
-43kDa
c
Fold Change of p-JNK/ t-JNK
3.0
2.5
2.0
1.5
1.0
0.5
0.0
0
10
30
60
10
30
60 min
Control
BMP-2
BMP-2 with TSG-6
p-JNK
t-JNK
β-actin
-54kDa
-46kDa
-45kDa

Figure 9. TSG-6 inhibits p38 and ERK1/2 signaling in THP-1 cells activated by a high BMP-2 concentration. THP-1 cells were treated with 5000 ng/ml of BMP-2 and/or 10 ng/ml of TSG-6 for 10, 30, or 60 minutes. Immunoblotting data were analyzed by the ratio of phospho-ERK1/2, phospho-p38, and phospho-JNK to total ERK1/2, total p38, and total JNK protein, respectively. (a) ERK1/2 signaling was activated by BMP-2 at 60 minutes, whereas TSG-6 treatment inhibited ERK1/2 signaling. (b) Also, p38 signaling was inhibited by TSG-6 treatment at a high BMP-2 concentrations. (c) JNK signaling had no significant influence on protein levels. Each bar represents the mean ± S.E. *$P<0.05$ compared with the control group, n=3.

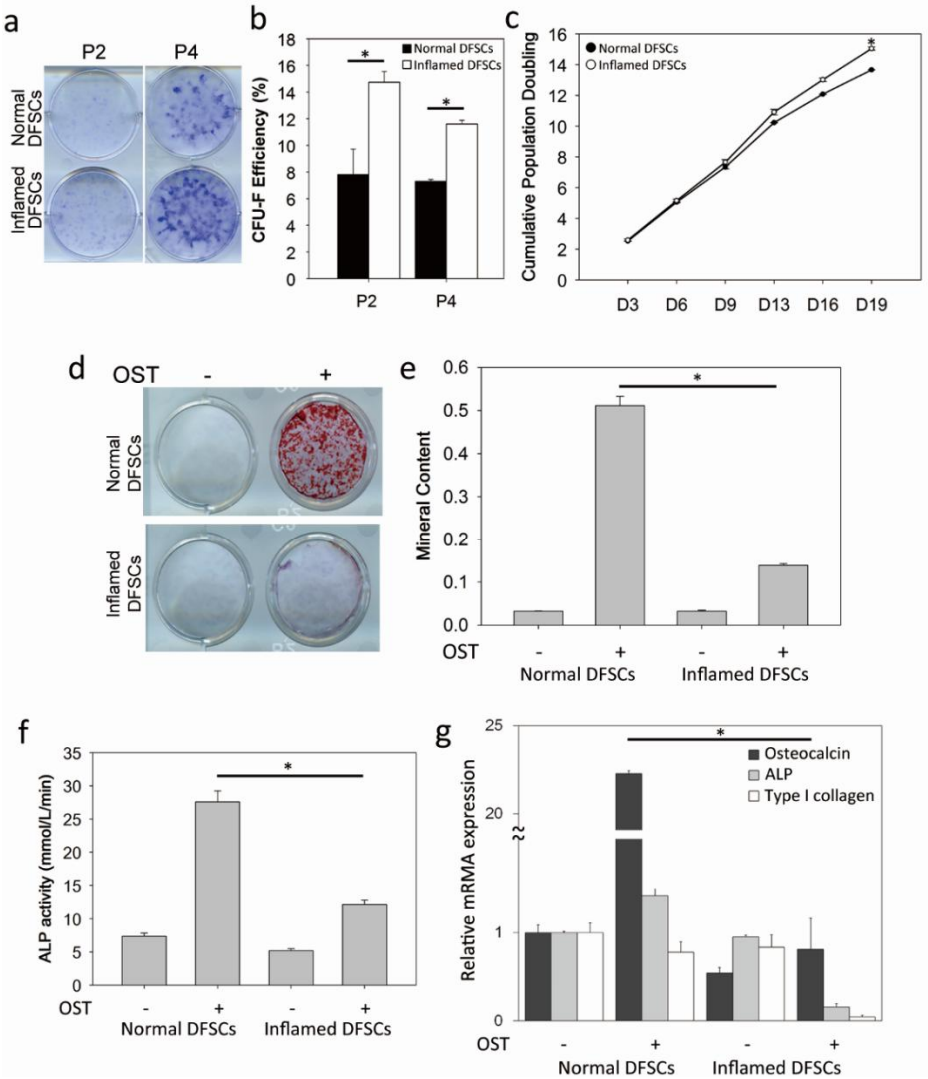
a
P2
P4
Normal DFSCs
Inflamed DFSCs
b
CFU-F Efficiency (%)
Normal DFSCs
Inflamed DFSCs
P2
P4
c
Cumulative Population Doubling
Normal DFSCs
Inflamed DFSCs
D3
D6
D9
D13
D16
D19
d
OST
-
+
Normal DFSCs
Inflamed DFSCs
e
Mineral Content
OST
Normal DFSCs
Inflamed DFSCs
f
ALP activity (mmol/L/min)
OST
Normal DFSCs
Inflamed DFSCs
g
Relative mRMA expression
Osteocalcin
ALP
Type I collagen
OST
Normal DFSCs
Inflamed DFSCs

Figure 10. Proliferation and osteogenic differentiation on normal and inflamed dental follicle stem cells (DFSCs). (a) DFSCs isolated both from normal and inflamed dental follicle were cultured in normal growth medium. Colony-forming assay was done by 1% crystal violet at passage 2 and 4. (b) Colonies, consisted of over 50 cells, were counted and calculated as a percentage of the number of seeded cells at passage 2 and 4. Inflamed DFSCs showed higher proliferative rate. (c) Cumulative population doubling of both normal and inflamed DFSCs was counted at day 3, 6, 9, 13, 16, and 19. There is significant proliferative difference between normal and inflamed DFSCs at day 19. (d) Calcium deposits formed by normal and inflamed DFSCs on osteogenic differentiation were stained by 40 mM alizarin red S solution at day 21. (e) Mineral contents dissolved by stained calcium deposits were dissolved by 20% methanol and 10% acetic acid. (f) ALPase activity, early osteogenic differentiation marker, was performed at day 7. (g) Real-time PCR showed that gene expression of osteocalcin, osteogenic marker, was down-regulated on inflamed DFSCs. Data represents the mean ± S.D. * $P<0.05$ (n=3).

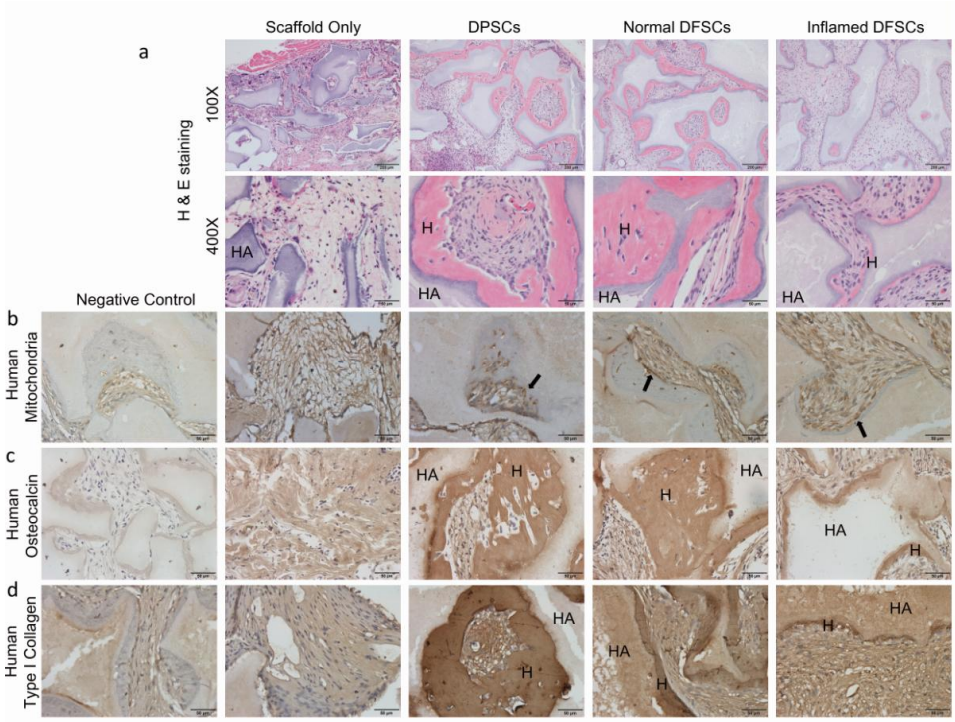

Figure 11. *In vivo* transplantation of normal and inflamed DFSCs. (a) H&E staining was performed to determine the hard tissue formed by transplanted normal and inflamed DFSCs with HA/TCP after 8 weeks transplantation on the backside of nude mice. Inflamed DFSCs showed significantly low hard tissue formation. (b) Human mitochondria was detected densely near hard tissue formation. (c, d) Hard tissue region were positively stained with human osteocalcin and type 1 collagen to confirm the hard tissue formed by transplanted normal and inflamed DFSCs. Each group showed significant different bone formation.

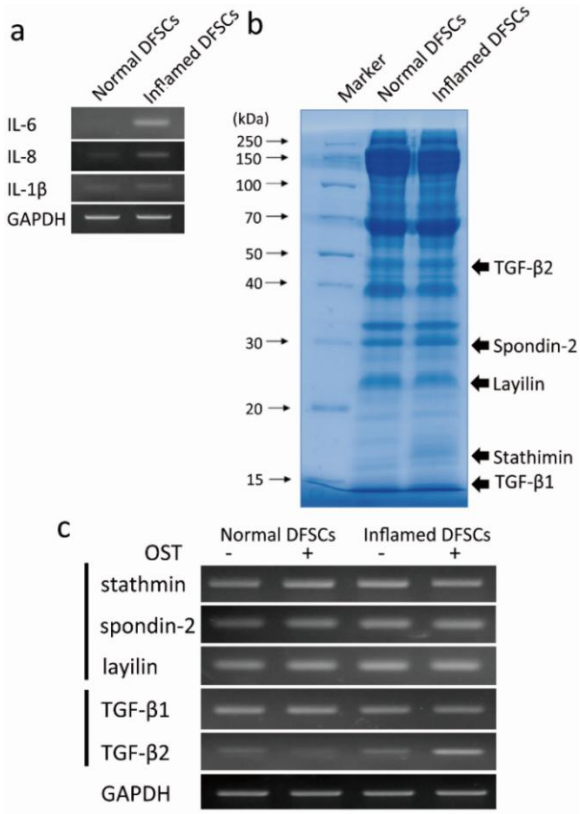

Figure 12. Gene profiling by RT-PCR. (a) Pro-inflammatory cytokines, IL-6, IL-8, and IL-1β, were detected DFSCs isolated from inflamed tissue. (b) Comparison of normal and inflamed dental follicle were performed in different bands of 1D-SDS-PAGE gel. (c) Among proteins with above Mascot score of 30 selected from LC-MS/MS analysis of normal and inflamed DFSCs, proteins related to osteogenic differentiation were selected. The gene expressions were determined by RT-PCR with specific primers at normal and inflamed DFSCs during osteogenesis. Different TGF-β2 gene expressions were detected between normal and inflamed DFSCs on osteogenesis.

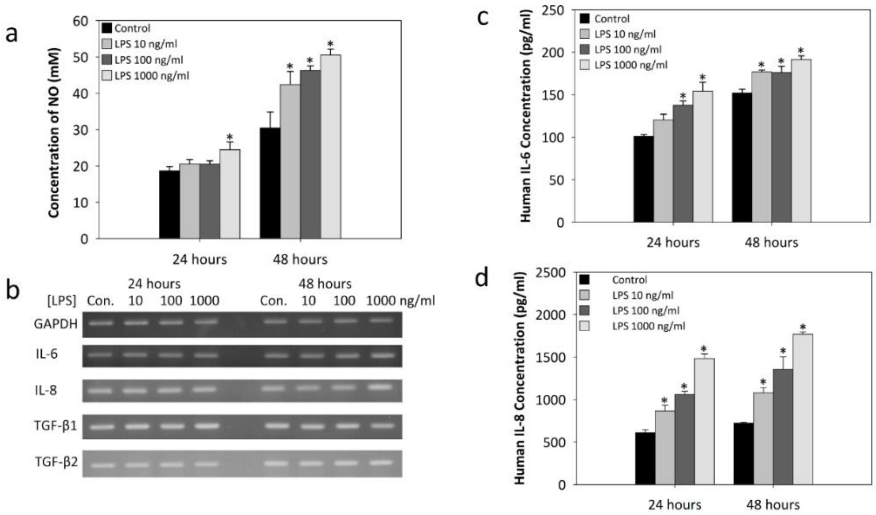

Figure 13. *Porphyromonas gingivalis* (*P.g.*)-derived LPS-induced inflammation mimics the inflammatory condition on DFSCs. (a) Cultured DFSCs were treated with various concentration, 10, 100, and 1000 ng/ml, of LPS to secret nitrate oxide (NO) for 24 and 48 hours. (b) Pro-inflammatory cytokines, IL-6 and IL-8, were increased in concentration dependent manners for 48 hours. However, there is no significant difference on gene expression of TGF-β1 and TGF-β2 on conditional medium with LPS treatment. (c, d) Protein levels of IL-6 and IL-8 were also increased with LPS treatment, respectively. Data represents the mean ± S.D. * $P<0.05$ (n=3).

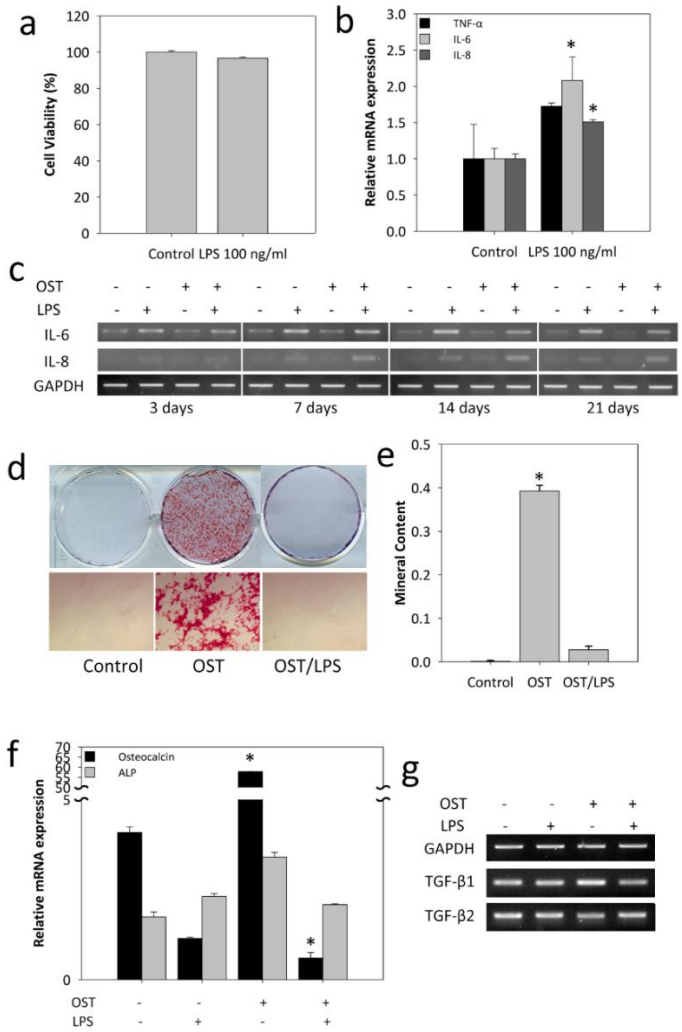
a
Cell Viability (%)
Control LPS 100 ng/ml
b
TNF-α
IL-6
IL-8
Relative mRNA expression
Control LPS 100 ng/ml
c
OST
LPS
IL-6
IL-8
GAPDH
3 days
7 days
14 days
21 days
d
Control
OST
OST/LPS
e
Mineral Content
Control OST OST/LPS
f
Osteocalcin
ALP
Relative mRNA expression
OST
LPS
g
OST
LPS
GAPDH
TGF-β1
TGF-β2

Figure 14. Down-regulation of osteogenic differentiation by *P.g.*- derived LPS on DFSCs. (a) MTT assay was performed to determine the cell viability on LPS treatment. There was no effect of LPS on cell viability at 100 ng/ml concentration. (b) Real-time PCR supported that pro-inflammatory cytokines, IL-6 and IL-8, were secreted on 100 ng/ml LPS treatment on conditional medium. (c) Gene expressions of IL-6 and IL-8 were also expressed during osteogenic differentiation with 100 ng/ml LPS treatment. (d, e) Calcium deposits during osteogenesis were inhibited with 100 ng/ml LPS treatment. Dissolved mineral contents were decreased about 4.5 fold compare to control without LPS treatment. (f) Osteocalcin gene were inhibited significantly. (g) Comparisons between TGF-β1 and TGF-β2 gene were performed by RT-PCR while differentiating osteogenic tissue with 100 ng/ml LPS treatment for 2 weeks. During osteogenesis, TGF-β1 expression were increased. However, TGF-β2 showed decreased expression. While treating LPS, TGF-β1 and TGF-β2 expression were changed inversely. LPS triggered higher TGF-β2 expression on osteogenesis. Data represents the mean ± S.D. * $P<0.05$ (n=3).

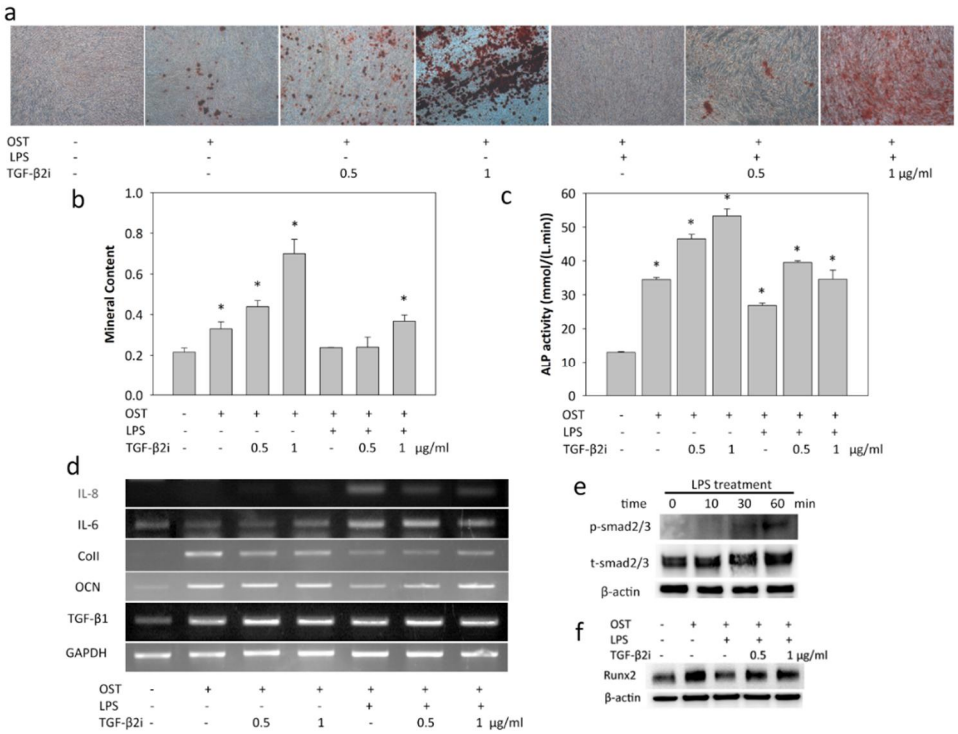
a
OST
LPS
TGF-β2i
0.5
1
1 μg/ml
b
Mineral Content
c
ALP activity (mmol/(L.min))
d
IL-8
IL-6
Coll
OCN
TGF-β1
GAPDH
e
LPS treatment
time 0 10 30 60 min
p-smad2/3
t-smad2/3
β-actin
f
Runx2
β-actin

Figure 15. Inhibition of TGF-β2 overcomes the down regulatory effect on bone formation suppressed by LPS. (a, b) Alizarin red S solution stained the calcium deposits while treating TGF-β2 inhibitor and LPS treatment at day 28. Dissolved mineral contents were decreased with LPS treatment. However, 1 μg/ml of TGF-β2 inhibitor can neutralize TGF-β2 secreted by LPS treatment. Interestingly, inhibition of TGF-β2 increased osteogenic differentiation of DFSCs. (c) ALPase activity also supported that inhibition of TGF-β2 increased early stage of osteogenesis of DFSCs. (d) With neutralizing TGF-β2 secreted by LPS-induced inflammation, pro-inflammatory cytokines, IL-6 and IL-8, were decreased. On the contrary, osteocalcin (OCN) and type 1 collagen (Col1) expression were increased with TGF-β2 inhibitor on LPS-induced inflammation. (e) 100 ng/ml LPS were activated smad2/3 signaling with over 30 minute treatment. (f) DFSCs activated with LPS for 30 minutes were treated with 0.5 μg/ml TGF-β2 inhibitor for 7 days on osteogenic differentiation. With TGF-β2 inhibitor, Runx2 expression were overcome. Data represents the mean ± S.D. * $P<0.05$ (n=3).

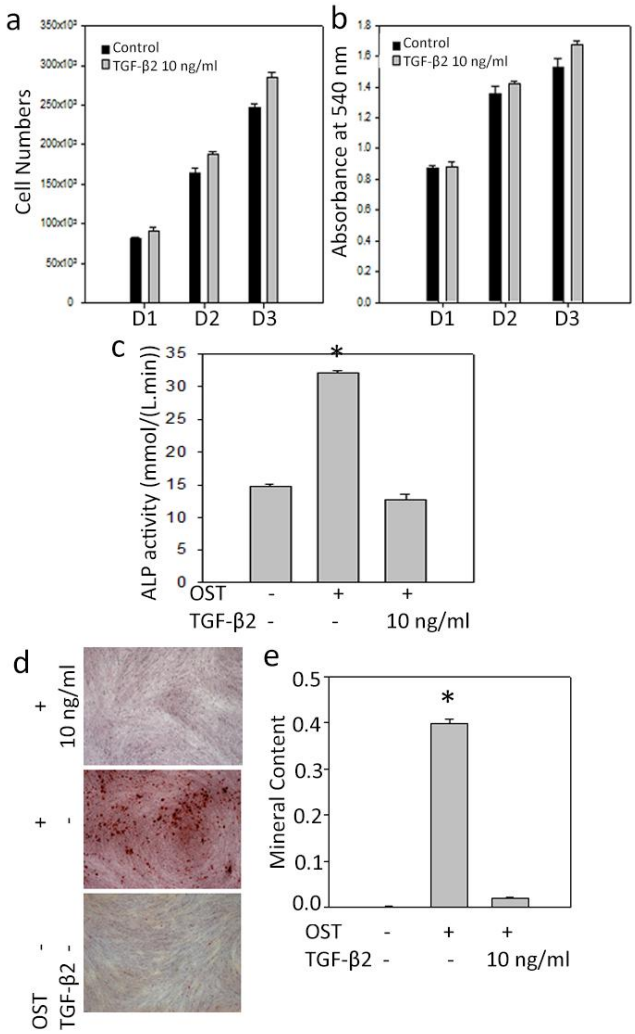

Figure 16. TGF-β2 affected the proliferation and osteogenic differentiation. (a,b) 10ng/ml of TGF-β2 increased the proliferation at day 1, 2 and 3. (c) The early osteogenic differentiation on DFSCs were inhibited with TGF-β2 treatment at day 7. (d,e) Alizarin red S staining showed the inhibition of osteogenic differentiation with 10 ng/ml TGF-β2. Data represents the mean ± S.D. * $P<0.05$ (n=3).

국문초록

서울대학교 대학원

치의과학과 치의재생생명공학 전공

엄 소 연

(지도교수 서병무)

1. 연구 목적

뼈형성은 염증에 의해서 파괴된 국소조직내 뼈와 주위 조직을 재건하는데 중요한 역할을 한다. 류마티스 관절염과 낭포성 섬유증, 치주염 등의 질환에서 보여지듯이, 염증 조건에서는 골분화도가 억제되는 것으로 알려져 있다. 이 논문에서는 중간엽 줄기세포의 일종인 치주인대줄기세포, 상악골유래 골수줄기세포, 치배줄기세포를 이용하여 염증과 골분화 사이의 관계를 살펴보고자 하였다.

2. 재료 및 방법

본 연구는 2 가지 연구소주제로 구성되어 있다. 제 1 소주제는 제 2형 골형성단백질(BMP-2)에 의해 유래된 염증반응이 중간엽줄기세포에서 분비된 TSG-6에 의해 조절되는 양상에 대해 조사하였다. BMP-2는 뼈와 관절의 발달 및 손상된 기관과 조직의 재생에 중요한 역할을 한다. 정형외과영역에서 사용되는 BMP-2의 0.5-1 mg/ml 의 농도 범위는 긴급한 수술이 필요할 정도로 심각한

수술후 후유증인 부종을 야기한다. 본 연구에서는 높은 농도의 BMP-2를 사용하여 염증세포인 THP-1 세포의 염증반응을 유도하고, 치주인대줄기세포와 상악골 유래 골수줄기세포의 골분화 억제가 나타남을 확인하였다. 골분화도는 ALP activity 및 alizarin red S 염색으로 확인하였으며, 단백질은 유세포분석기, 효소면역측정법, 웨스턴블럿, 면역세포화학을 통하여 분석하였다. 유전자 발현 양상은 중합효소 연쇄반응을 이용하여 확인하였다.

두번째 소주제는 치주관련 질환에서 치조골과 치주조직을 재건하는데 효과적인 치배의 발달과정중 발견되는 치배조직내 줄기세포에 초점을 맞추었다. 감염된 치주조직 내 박테리아 감염에 의해 주변조직의 골파괴가 관찰된다. 그러나 염증환경과 골형성 간의 관계는 아직 명확하게 밝혀지지 않았다. 골분화도는 ALP acitiviy와 alizarin red S 염색을 통해 알아보았고, *in vivo* 이식후, 조직염색을 통해 줄기세포의 골분화도를 확인하였다. 단백질 프로파일링 분석 및 액체크로마토그래피를 통해 세포간 비교실험을 진행하였으며, LPS 처리를 통한 염증유도 진행 후, 유전자발현량을 중합효소 연쇄반응을 이용해 알아보았다.

3. 연구결과

첫 번째 소주제의 연구결과, 높은 농도의 BMP-2는 중간엽줄기세포의 초기 골분화를 억제하였다. 중간엽 줄기세포만 골분화 했을 때에 비해 염증세포인 THP-1와 중간엽 줄기세포의

공배양시, 후기 골분화가 억제되는 것을 확인하였다. 또한 높은 농도의 BMP-2 처리시 THP-1 세포에서 염증 사이토카인을 분비하고 중간엽줄기세포인 치주인대줄기세포와 골수줄기세포에서 TSG-6의 분비를 확인하였다. THP-1 세포와 공배양된 중간엽줄기세포의 항염증반응과 유사하게, THP-1 세포에 TSG-6의 처리시, 염증 사이토카인인 IL-1β 의 발현이 감소하였다. 그러므로 고용량의 BMP-2가 THP-1 세포에서 염증 사이토카인을 분비하고, 이때 야기된 염증반응에 의해 골분화의 억제가 야기함을 확인하였다. 반면에 중간엽줄기세포에서 분비된 TSG-6는 염증반응을 p38와 ERK in the mitogen-activated protein kinase (MAPK) 경로를 통해 억제하였다.

두 번째 파트의 연구에서는 감염된 조직에서 추출된 치배 내 줄기세포를 골분화 한 결과 ALP acitiviy와 alizarin red S 염색을 통해 정상 치배줄기세포보다 골분화가 억제됨을 확인하였다. 또한 감염된 치배줄기세포 *in vivo* 이식시, 골형성이 억제되는 양상을 보였다. 단백질 프로파일링 분석 및 액체크로마토그래피를 통해 정상 및 염증유래 치배줄기세포를 비교 분석한 결과, TGF-β2의 발현량이 크게 차이 남을 확인하였다. Porphyromonas gingivalis (P.g.) 유래 LPS를 사용해, 세포에서의 염증유도를 진행한 결과 LPS가 처리된 치배줄기세포의 경우 골분화의 억제와 함께 TGF-β1 발현이 억제되었고 TGF-β2는 증가하였다. TGF-β2의 억제제 처리시 치배줄기세포에서 alizarin red S 염색 및 ALP

activity가 증가되었고 TGF-β1의 발현이 높게 나타났다. 임상적 및 실험적 상황에서 염증조건에서 TGF-β2의 발현이 증가되었으며 골형성이 억제됨을 확인하였다.

4. 결론

이상의 결과를 종합하면, 염증환경은 중간엽줄기세포의 골분화도에 영향을 미치며 염증상황에서 중간엽줄기세포는 TGF-β2에 의해서 골분화능이 억제된다. 또한 염증상황에서 중간엽줄기세포는 항염증사이토카인인 TSG-6을 분비하여 염증반응을 억제하고 및 골분화도를 억제를 역전시키는 것으로 보여진다. 중간엽줄기세포의 염증 및 골형성 사이의 관계를 이해함으로써, 향후 치아유래 줄기세포의 재생의학적 측면에서의 임상적인 활용에 도움이 될 수 있을 것으로 기대한다.

주요어: 치주인대줄기세포, 골수줄기세포, 치배줄기세포, 뼈재생, 염증, BMP-2, TSG-6, TGF-β2

학번: 2011-23827